# Ageing of an oscillator due to frequency switching

Carles Bonet[a], Mike R. Jeffrey[b,*], Pau Martín[a], Josep M. Olm[c]

[a]*Department of Mathematics, Universitat Politècnica de Catalunya, Spain*
[b]*Department of Engineering Mathematics, University of Bristol, UK*
[c]*Department of Mathematics & Institute of Industrial and Control Engineering, Universitat Politècnica de Catalunya, Spain*

**Abstract**

If an oscillator is driven by a force that switches between two frequencies, the dynamics it exhibits depends on the precise manner of switching. Here we take a one-dimensional oscillator and consider scenarios in which switching occurs either: (i) between two driving forces which have different frequencies, or (ii) as a single forcing whose frequency switches between two values. The difference is subtle, but its effect on the long term behaviour is severe, and occurs because the expressions of (i) and (ii) are linear and nonlinear, respectively, in terms of a discontinuous quantity (e.g. a sign or Heaviside step function) that represents the switch between frequencies. In scenario (i) the oscillator can be described as a *Filippov system*, and we will show it has a stable periodic orbit. In scenario (ii) the oscillator exhibits *hidden dynamics*, which lies outside the theory of Filippov's systems, and causes the system to be increasingly (as time passes) dominated by sliding along the frequency-switching threshold, and in particular if periodic orbits do exist, they too exhibit sliding. We show that the behaviour persists, at least asymptotically, if the systems are regularized (i.e. if the switch is modelled in the manner of (i) or (ii) but with a smooth rather than discontinuous transition).

*Keywords:* nonsmooth, Filippov, hidden dynamics, piecewise, ageing, switching, mixed-mode

*Corresponding author: Mike R. Jeffrey
*Email addresses:* carles.bonet@upc.edu (Carles Bonet), mike.jeffrey@bristol.ac.uk (Mike R. Jeffrey), p.martin@upc.edu (Pau Martín), josep.olm@upc.edu (Josep M. Olm)

## 1. Introduction

The theory of piecewise-smooth dynamical systems enables the study of how systems behave at 'switching manifolds' where they suffer discontinuities. Filippov showed in [9] how to study such systems by forming a differential inclusion across the discontinuity, creating a set-valued problem from which one may select a range of possible solutions. Interest has grown in whether these different possible solutions have practical relevance, whether they behave differently, and what theoretical or practical criteria can be drawn to choose between them, particularly in light of their growing range of applications (see e.g. [7, 16, 28] for broad overviews).

To illustrate the issues that arise in looking beyond so-called *Filippov systems*, a simple oscillator was proposed in [15, 16] in which the appropriate choice of solutions at the discontinuity was unclear. The model takes the form of a second order oscillator,

$$\dot{y} = -ay - z - \sin(\pi\omega t) \ , \qquad \dot{z} = y \ , \tag{1}$$

where the dot denotes the derivative with respect to $t$, where the sinusoidal forcing switches between two frequencies, some $\omega = \omega_+$ for $y > 0$ and $\omega = \omega_-$ for $y < 0$. Solving this system either numerically or analytically proves challenging, and centers around how the discontinuity at $y = 0$ is handled. In particular we may place the discontinuity either in the size of the forcing term, so it switches between two sinusoids with different frequencies,

$$\sin(\pi\omega t) = \tfrac{1}{2}(1+\lambda)\sin(\pi\omega_+ t) + \tfrac{1}{2}(1-\lambda)\sin(\pi\omega_- t) \ , \tag{2a}$$

or place the discontinuity in the frequency of the forcing directly, as

$$\sin(\pi\omega t) = \sin\left(\left\{(1+\lambda)\omega_+ + (1-\lambda)\omega_-\right\}\frac{\pi t}{2}\right) \ , \tag{2b}$$

both in terms of a discontinuous quantity $\lambda = \mathrm{sign}(y)$, called a *switching multiplier*. The sign function takes values $+1$ for $y > 0$, $-1$ for $y < 0$, and $\lambda \in (-1, +1)$ for $y = 0$. The two models (2a) and (2b) are therefore equivalent for $y \neq 0$, but, as observed in [15], they differ crucially in the dynamics they generate at $y = 0$, and this utterly changes their global behaviour.

Why this happens was left as an open challenge in [15]. The dynamics of the oscillator with this frequency switching is complex and highly sensitive, and is easily mis-calculated in numerical simulations. This means that the difference between the models (2a) and (2b) may not easily reveal itself.

Our aim here is to begin investigating the qualitative dynamical features that organize the true behaviour of the system, and to see why they make simulating it so challenging.

Oscillators with discontinuities have been an important application in the general development of piecewise-smooth dynamics, principally in dry-friction oscillators [25, 12, 18, 1], impact oscillators [26, 11, 10, 14], and industrial applications abound in problems such as valves [13], drills [17], and braking [6, 29]. Approaches to study these involve either hybrid systems or complementarity constraints [20, 4, 7], or Filippov's convex approach [7, 18, 19].

In such a system one can define solutions in $y > 0$ and $y < 0$ in the usual way for a differentiable system, while solutions on $y = 0$ can be defined in a number of possible ways that we discuss below. Solutions of the complete system are then obtained by matching solutions in these three regions, $y > 0$, $y < 0$, and $y = 0$, by simple concatenation (in a manner that preserves the direction of time along any solution).

Whatever methods are used to define the solutions at the discontinuity (on $y = 0$), of course, the solutions obtained are inescapably non-unique. Although it is a standard result of dynamical systems theory that uniqueness cannot be guaranteed if its differential equations have discontinuities (see e.g. [9, 24, 21, 15]), little is currently understood about what physical meaning, if indeed any, the infinity of possible solutions might have. The system (1) was conceived to illustrate a simple system where this non-uniqueness would be observable, requiring careful simulation and considered solution methods.

Filippov's approach to handling the discontinuity at $y = 0$ consists of forming a differential inclusion across the discontinuity, thus creating a convex set of possible trajectories across it, yielding solutions that can cross through or slide along switching manifolds in a largely unique manner (up to certain singularities, see e.g. [5]), and an extensive theory of their existence, uniqueness, stability and bifurcations now exists (see e.g. [9, 7, 19]).

For systems involving nonlinear functions of a discontinuous term, as we have in (2b), something beyond Filippov's analysis is required to define a system and its solutions. The approach developed in [15, 16], where this oscillator problem was posed, consists of blowing up the switching manifold $y = 0$ into a *switching layer* $y \in [-\varepsilon, \varepsilon]$, by letting $y = \varepsilon\lambda$ for $|y| \leq \varepsilon$ (while $\lambda = \text{sign}(y)$ for $|y| > \varepsilon$), for some parameter $\varepsilon > 0$, and taking the limit $\varepsilon \to 0$. This allows us to study the dynamics of the multiplier $\lambda$ on the layer interval $\lambda \in [-1, +1]$ even as $\varepsilon \to 0$. However, this dynamics differs depending whether the switch in the system is expressed by (2a) or (2b).

To emphasize that the different behaviours obtained using (2a) or (2b)

are not an artefact of the blow-up approach proposed in [15, 16], we will here use the Sotomayor-Teixeira regularization method [27]. Though the two methods are shown to yield equivalent dynamics in [23], Sotomayor-Teixeira regularization has been more widely studied to date, and involves the more standard notion of smoothing out the discontinuity by replacing $\lambda$ in (2) with a smooth *transition* function $\lambda \mapsto \phi(y/\varepsilon)$, where $\phi$ is monotonic and differentiable for small $\varepsilon > 0$, such that $\phi(y/\varepsilon) \to \text{sign}(y)$ as $\varepsilon \to 0$. This results in a smoothly differentiable system, therefore permitting the use of many standard results of dynamical systems theory to study it, in particular the geometric singular perturbation analysis we will make use of here.

To gain insight into the complex dynamics of the system (1)-(2), we propose here to first study a simplified first order oscillator,

$$\dot{y} = -ay - \sin(\pi\omega t) \ , \tag{3}$$

along with the switching rules (2). This exhibits most of the key features that make (1) with (2) so challenging, and that original system will then be analysed in follow-up work.

As well as being lower dimensional, the first order system (3) has the advantage of representing a simple electronic RL circuit, as shown in Figure 1. A circuit with current $i$, driven through a resistance $R$ and inductance $L$ by an alternating current voltage source $V(t)$, satisfies the equation $V(t) = L\frac{di}{dt} + Ri$, or

$$\frac{di}{dt} = -\frac{R}{L}i + \frac{V(t)}{L} \ . \tag{4}$$

By letting $\frac{R}{L} = a$ and $V(t) = -L\sin(\pi\omega t)$, we obtain (3). If the frequency of

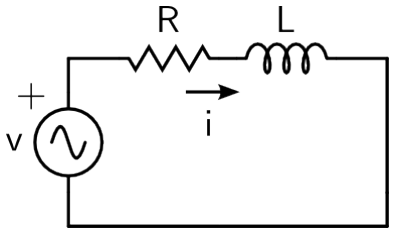


Figure 1: A resistor-inductor circuit with an alternating current voltage source.

the alternating current source is then switched between values $\omega_\pm$ whenever the current reverses direction (when $i$ passes through zero), the question of whether this is modelled by (2a) or (2b) becomes one of the precise control

feedback between the current and the frequency switch. A linear controller switching between $\omega = \omega_\pm$ with a small hysteresis will be well modelled by (2a), while a variable frequency voltage source should be well modelled by (2b), as proven in [2]. We shall see that (2a) leads to stable oscillations, while (2b) causes the system to age and become unable to alternate its current, i.e. $i$ becomes fixed in $i \leq 0$.

In this paper we shall show that the 'linear switching' system, governed by (2a), has relatively simple dynamics dominated by a stable period 4 orbit. For small damping parameter $a$ the period 4 orbit crosses transversally between the two frequency modes and is asymptotically stable (Theorem 1 in Section 3). For large $a$ the period 4 orbit has a segment of sliding along the switching manifold $y = 0$, and nearby orbits collapse onto it in finite time (Theorem 2 in Section 3).

The 'nonlinear switching' system governed by (2b), exhibits more complex dynamics. There are no periodic orbits that switch transversally between frequencies (Theorem 3 in Section 3.2), and indeed it becomes impossible for solutions of (3) to switch frequencies at late times (Theorem 5 in Section 3.2). A period 4 orbit emerges (Theorem 4 in Section 3.2) that exists only in the lower frequency state and on the switching manifold, but under regularization is revealed to penetrate less and less deeply into the 'switching layer' on each period. We can summarize these by saying that the nonlinear system exhibits:

- ageing – the multiplier $\lambda$ interacts in a non-trivial way with the independent variable $t$ in (2b), such that the dynamics at $y = 0$ changes qualitatively, and irreversibly, as $t$ increases.

- multiple timescale phenomena – the nonlinear dependence on $\lambda$ in (2b) creates intricate layering of slow manifolds governing the behaviour at $y = 0$.

In (3) these have two main effects, meaning that the later a trajectory reaches $y = 0$, the longer it may remain there, and also meaning the system asymptotes to but never exactly achieves periodicity. This is further complicated by the system's slow manifolds becoming more crowded as time increases, requiring deeper analysis than typical Fenichel theory to prove the persistence of behaviours under regularization. For the full system (1) our preliminary work suggests that all of these phenomena are further complicated by relaxation oscillations and mixed mode oscillations, which will be explored in follow-up work.

Notice that one key effect of the discontinuity lying inside or outside the argument of the sine function in (2) is that the linear switching system based on (2a) is 4-periodic system, while the nonlinear system based on (2b) is not. As a result the former possesses a 4-periodic orbit while the latter does not.

We shall show that the distinction between the linear and nonlinear systems from (2a) and (2b) remains under regularization, with the periodic orbits of the linear switching system remaining periodic (Theorem 6 and Theorem 7 in Section 4.1), while in the nonlinear system there persists an aperiodic oscillation lying close to that of the non-regularized system (Theorem 8 in Section 4.2). We shall also see that, for the nonlinear system, a regularization is necessary to rigorously define its solutions, and to distinguish between the many different sliding solutions that are possible.

Our approach will be as follows. In Section 2 we carry out a preliminary analysis and introduce the definitions of solutions for the discontinuous systems. In Section 3 we study the key dynamical features, such as periodic orbits, that distinguish the linear and nonlinear systems. Then in Section 4 we study the regularization of the two systems. Some concluding remarks are made in Section 5.

## 2. Preliminaries: dynamics of the piecewise-smooth system

Let us begin by re-writing (3) as an autonomous piecewise-smooth system,

$$\dot{x} = 1, \tag{5a}$$
$$\dot{y} = -ay - f_i(x, \lambda), \tag{5b}$$

where $a > 0$. The forcing $f_i$ takes one of the two forms from (2), and for simplicity we now set $\omega = \omega_+ = 3/2$ for $y > 0$ and $\omega = \omega_- = 1/2$ for $y < 0$. Any pair of commensurable frequencies would give rise to the same behaviour. The functions $f_L(x, \lambda)$ given by (2a), and $f_R(x, \lambda)$ given by (2b), can then be more concisely written as

$$f_L(x, \lambda) = [1 + (1 + \lambda)\cos \pi x] \sin \tfrac{\pi x}{2} \ , \tag{6a}$$
$$f_N(x, \lambda) = \sin\left(\pi x(1 + \tfrac{1}{2}\lambda)\right) \ , \tag{6b}$$

where $\lambda = \text{sign}(y)$, and where $i = L$ or $N$ indices the linear or nonlinear models of switching, respectively. Again we specify the sign function as taking values $+1$ for $y > 0$, $-1$ for $y < 0$, and $\lambda \in (-1, +1)$ for $y = 0$. For

$y \neq 0$ both $f_L$ and $f_N$ give $f_i(x, \pm 1) = \sin(\pi\omega_\pm x)$, with the '$\pm$' coinciding with the sign of $y$.

We will first sketch out the key regions and features separating different modes of dynamics in Section 2.1, then give expressions for solutions in the two frequency modes $\omega = \omega_\pm$ in Section 2.2. Using these we then seek periodic orbits of the two alternative systems described by (6a) and (6b) in Section 3.

*2.1. Regions and key features*

Let $S_\pm$ denote the upper and lower half-planes of $(x, y) \in \mathbb{R}^2$, i.e.

$$S_\pm = \left\{(x, y) \in \mathbb{R}^2 \ : \ \pm y > 0\right\} \ , \tag{7}$$

with the boundary or *switching manifold* between them denoted

$$S_0 = \left\{(x, y) \in \mathbb{R}^2 \ : \ y = 0\right\} \ . \tag{8}$$

We denote the closure of $S_\pm \cup S_0$ as $\overline{S}_\pm$. The switching manifold $S_0$ itself can be divided into regions where the vector fields in $S_\pm$ point towards or away from $S_0$. Since the subsystems on $S_+$ and $S_-$ are periodic, repeating every $\Delta x = 4/3$ and $\Delta x = 4$ respectively, it is enough to define these regions on the interval $0 \leq x \leq 4$. We define

$$S_{0A} = \left\{(x, y) \in S_0 \ : \ x \in (\tfrac{8}{3}, \tfrac{10}{3})\right\} \ , \tag{9a}$$
$$S_{0R} = \left\{(x, y) \in S_0 \ : \ x \in (\tfrac{2}{3}, \tfrac{4}{3})\right\} \ , \tag{9b}$$
$$S_{0C} = \left\{(x, y) \in S_0 \ : \ x \in (0, \tfrac{2}{3}) \cup (\tfrac{4}{3}, 2) \cup (2, \tfrac{8}{3}) \cup (\tfrac{10}{3}, 4)\right\} \ . \tag{9c}$$

As illustrated in Figure 2, these portion the switching manifold into:

- *attracting regions* $S_{0A}$, where the fields in $S_\pm$ point towards $S_0$,
- *repelling regions* $S_{0R}$, where the fields in $S_\pm$ point away from $S_0$, and
- *crossing regions* $S_{0C}$ everywhere else.

The boundaries between these are places where the vector fields in $S_\pm$ are tangent to $S_0$, i.e. where $\dot{y} = y = 0$. This happens on two sets (associated with the two frequency values $\omega = \omega_\pm$), given by

$$T_+ = \{(x, y) \in S_0 \ : \ x = 2n/3\} \ , \tag{10a}$$
$$T_- = \{(x, y) \in S_0 \ : \ x = 2n\} \ , \tag{10b}$$

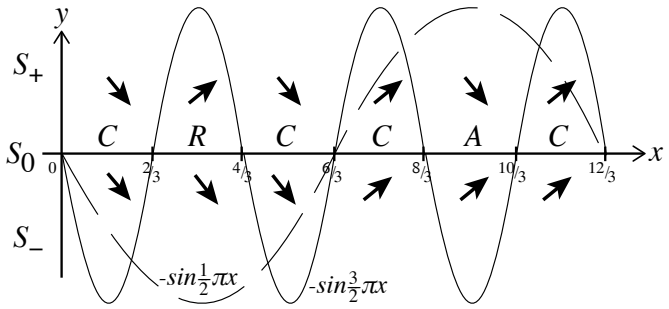


Figure 2: The half-planes $S_\pm$ and the switching manifold $S_0$, including the regions of attracting ($A$) and repelling ($R$) sliding, and crossing ($C$). The function $-\sin(\omega\pi x)$ for $\omega = \frac{1}{2}, \frac{3}{2}$, are also shown, along with the directions of the vector fields in $S_\pm$.

such that $\dot{y} = \sin(\pi\omega_+ x) = 0$ on $T_+$ and $\dot{y} = \sin(\pi\omega_- x) = 0$ on $T_-$.

Within any of the regions $S_\pm$, and $S_{0A}$, $S_{0R}$, $S_{0C}$, each system is differentiable and has standard solutions (as we show below these can be simply written as $x(t) = x_0 + t$, $y(t) = 0$, on $S_0$, and by $x(t) = x_0 + t$, $y(t) = Y_\pm(x(t), x_0)$ in $S_\pm$ for functions $Y_\pm$ that we give in Section 2.2). These solutions are then matched between regions to obtain solutions over the full space. Solutions that evolve along $S_0$ are called *sliding modes*, and in the theory of Filippov these evolve only along $S_{0A}$ or $S_{0R}$ [9], and in the extended theory provided by *hidden dynamics* these can evolve also along $S_{0C}$ [16].

So let us begin by defining sliding modes, which evolve along a *sliding manifold* on $S_0$, showing how they differ for the linear system that makes use of (6a), versus the nonlinear system that makes use of (6b).

We can make this more precise using the notion of *sliding manifolds*. A sliding manifold as defined in [16] is a set of points on $S_0$ where the vector field propagates solutions along $S_0$, that is where $y = 0$ and $\dot{y} = 0$. Places where $\frac{\partial \dot{y}}{\partial \lambda} < 0$ create attracting sliding manifolds, which we label $\Lambda^L$ and $\Lambda^N$ in the linear and nonlinear systems, respectively, and these will be our main concern. (Places where $\frac{\partial \dot{y}}{\partial \lambda} > 0$ create repelling sliding manifolds, which will be of less interest).

**Definition 1.** *We define the sliding manifold in the linear system, based on* (6a)*, as*

$$\begin{aligned}\Lambda^L &:= \cup_{n\in\mathbb{N}} S_{0A} + \{(4n, 0)\} \\ &= \cup_{n\in\mathbb{N}} \left\{(x, y) : y = 0,\ x \in \left(\tfrac{8}{3} + 4n, \tfrac{10}{3} + 4n\right)\right\}. \end{aligned} \tag{11}$$

*We define the sliding manifold in the nonlinear system, based on* (6b)*, as*

$$\Lambda^N := \cup_{n\in\mathbb{N}}\Lambda_n^N = \cup_{n\in\mathbb{N}} \left\{(x,y) : y = 0,\ x \in \left(\tfrac{4n}{3}, 4n\right)\right\}. \tag{12}$$

The set $\Lambda^L$ is the set of points on $S_0$ that is attracting with respect to the dynamics in $y > 0$ and $y < 0$. The set $\Lambda^N$ satisfies a more general notion of attractivity, and their distinction will become clear when we consider regularization in Section 4.1 and Section 4.2.

Notice that the sets $\Lambda_n^N$ are not disjoint, unlike the sets that make up $\Lambda^L$. Because the sets $\Lambda_n^N$ are not disjoint, a point $p \in \Lambda^N$ can belong in general to several $\Lambda_n^N$ with different $n$. The appropriate value of $n$ along a given solution is determined by the dynamics, using definition 5 below.

We use these manifolds to define solutions of the systems as follows. First note that the dynamics (5a) on the sliding manifolds $\Lambda^L$ or $\Lambda^N$ is given, since $y = \dot{y} = 0$ on $S_0$, by

$$\dot{x} = 1\ , \qquad y(t) = 0\ . \tag{13}$$

Now consider the linear system.

**Definition 2.** *Let $p = (x_0, 0) \in \Lambda^L$, and let $n$ be such that $x_0 \in (\frac{8}{3} + 4n, \frac{10}{3} + 4n)$. The solution through $p$ is given by* (13) *while $x$ remains in $(\frac{8}{3} + 4n, \frac{10}{3} + 4n)$.*

**Definition 3.** *Let $p \in S^+ \cup S^- \cup \Lambda^L \cup (\cup_{n\in\mathbb{N}}(S_{0C} + \{(4n, 0)\}))$. The solution of system* (5) *through $p$ in the linear case* (6a) *is defined as follows.*

1. *If $p \in S^+ \cup S^-$, the solution is given by the flow of the corresponding vector field, until it reaches $S_0$. Then it follows one of the following.*
2. *Let $p \in (\cup_{n\in\mathbb{N}}(S_{0C} + \{(4n, 0)\}))$. Assume that $\dot{y} > 0$ $[\dot{y} < 0]$ at $p$. The solution that passes through $p$ at $t = 0$ follows the upper [lower] vector field in $y > 0$ $[y < 0]$ for small $t > 0$, and follows the lower [upper] vector field in $y < 0$ $[y > 0]$ for small $t < 0$.*
3. *If $p \in \{(x, y) :\ x \in (\frac{8}{3}+4n, \frac{10}{3}+4n),\ y = 0\} \subset \Lambda^L$, the solution through $p$ is given by $\dot{x} = 1$, $y = 0$ until it reaches the point $(\frac{10}{3} + 4n, 0)$. There it is matched with the solution of the upper vector field that starts at $(\frac{10}{3} + 4n, 0)$.*

**Remark 1.** *By Definition 3 the flow through a point $(x, 0) \in \Lambda^L$ may not be unique, because any solution through a point in $x \in (\frac{8}{3} + 4n, \frac{10}{3} + 4n) \subset \Lambda^L$ will slide and exit the switching manifold through the point $(\frac{10}{3} + 4n, 0)$. We exclude from this definition any solutions through the repelling part of the switching manifold, which will not be of interest here.*

We define solutions in the nonlinear case similarly.

**Definition 4.** *Let $p = (x_0, 0) \in \Lambda^N$, and let $n \geq 1$ be such that $x_0 \in \Lambda_n^N = (4n/3, 4n)$. The solution through $p$ is the one given by* (13) *while $x$ remains in $\Lambda_n^N$.*

**Definition 5.** *Let $p = (x_0, y_0) \in S^+ \cup S^- \cup \{(x, 0) : \ x \in (0, \frac{2}{3})\}$. The solution through $p$ of system* (5) *in the nonlinear case* (6b) *is defined as follows.*

1. *If $p = (x_0, 0)$, with $x_0 \in (0, \frac{2}{3})$, the solution is given by* (2) *of Definition 3.*
2. *If $p \in S^+$. Let $\varphi_+(t, p)$ be the flow of the upper vector field through $p$. Assume that there exists $t_0 > 0$ such that $\varphi_+(t_0, p) \in S_0$, $\varphi_+(t, p) \in S^+$, for $t \in (0, t_0)$ and $\pi_x\varphi_+(t_0, p) \in (4n/3, (4n + 2)/3)$, for some $n \geq 1$. Then the solution slides, with $\dot{x} = 1$, $\dot{y} = 0$, until it reaches $(4n, 0)$, where it is matched with the solution of the lower vector field that starts at $(4n, 0)$.*
3. *If $p \in S^-$. Let $\varphi_-(t, p)$ be the flow of the lower vector field through $p$. Assume that there exists $t_0 > 0$ such that $\varphi_-(t, p) \in S^-$, for $t \in (0, t_0)$ and $\pi_x\varphi_-(t_0, p) \in (4n - 2, 4n)$, for some $n \geq 1$. Then the solution slides, following* (13)*, until it reaches $(4n, 0)$, where it is matched with the solution of the lower vector field starting from $(4n, 0)$.*

**Remark 2.** *In this definition we are excluding a measure* 0 *set of orbits that enter $S_0$ at the point points $((4n + 2)/3, 0)$ for $n \in \mathbb{N}$ (these can be studied by the regularization methods we develop in Section 4, but are beyond our interest here).*

**Remark 3.** *In the nonlinear case the roles played by the crossing regions $S_{0C}$ and sliding regions $S_{0A}$ or $S_{0R}$ is more complex than in the linear case, the latter following the more simple dynamics of a 'Filippov system' [9]. This will become clearer in the regularization of the system in Section 4.2.*

When studying periodic solutions the following distinction will be useful.

**Definition 6.** *A periodic solution of* (5) *is a* sliding periodic orbit *if part of it lies on the sliding manifold $\Lambda^i$, $i = L, N$, otherwise it is a* non-sliding periodic orbit.

These behaviours are illustrated in Figure 3 for the linear switching system.

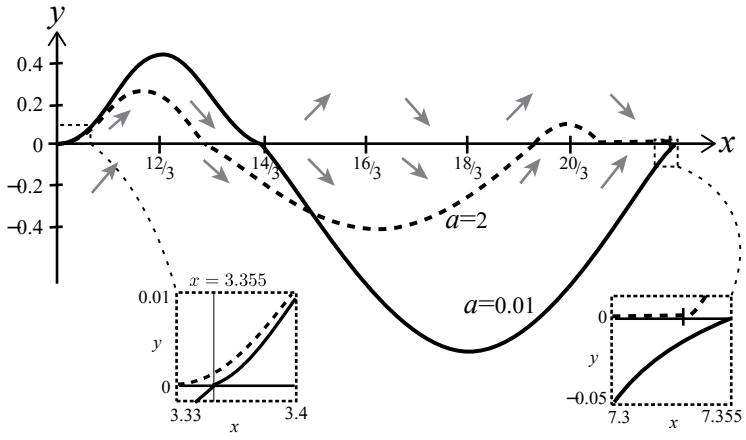


Figure 3: Examples of two periodic orbits for the linear switching system for $a = 0.01$ and $a = 2$ as labelled. A sliding 4-periodic solution (dotted) is shown passing through point $(x, y) = \left(\frac{10}{3}, 0\right)$ which lies on the right hand side extremum of the first region $S_{0A}$ in $x > 0$, and returning to the next region $S_{0A}$ after two crossings. A non-sliding 4-periodic solution (full curve) is also shown starting at $(x, y) = (3.355, 0)$ and returns to $(x, y) = (7.355, 0)$ after one crossing (both in regions $S_{0C}$). Magnifications of the solutions at the start and end of this interval are shown. Arrows indicate the directions of the vector fields in $S_{\pm}$. (Values given to 4 sig. figs.)

Explicit expressions can be found for the partial solutions of (5) in the two separate half planes $S_{\pm}$, and we begin by finding these in Section 2.2. These will be the same whether we use (6a) or (6b) (and will still apply in Section 4 to the regularized system), and we use them to find periodic orbits in Section 3.

*2.2. Orbits in the two frequency modes, $S_{\pm}$*

Let $y = Y_{\pm}(x, x_i)$ denote a solution of (5) that starts from a point $(x_i, 0) \in S_0$, so that $Y_{\pm}(x_i, x_i) = 0$, and the '$\pm$' denotes whether the orbit departs $S_0$ into $S_+$ or $S_-$ (orbits remaining on $S_0$ will be considered in Section 3).

The evolution in either half plane $S_{\pm}$ is governed simply by (5) with $\lambda = \pm 1$ in $S_{\pm}$. Solving in each subsystem separately gives

$$\begin{aligned} Y_{\pm}(x, x_i) = & \frac{1}{\omega_{\pm}^2 \pi^2 + a^2} \Big[ \; \omega_{\pm} \pi \cos(\omega_{\pm} \pi x) - a \sin(\omega_{\pm} \pi x) \; + \\ & e^{-a(x - x_i)} \left\{ a \sin(\omega_{\pm} \pi x_i) - \omega_{\pm} \pi \cos(\omega_{\pm} \pi x_i) \right\} \Big], \end{aligned} \tag{14}$$

with $x \in [x_i, x_{i+1}]$, where $x_{i+1}$ is the next point instersection point with $S_0$, i.e. at which $Y_{\pm}(x_{i+1}, x_i) = 0$ and $x_{i+1} > x_i$.

Setting $\bar{x} = x - x_i$ in (14) and grouping trigonometric terms yields $Y_\pm(x_i + \bar{x}, x_i) = y_\pm(\bar{x}, x_i)$, where

$$y_\pm(\bar{x}, x_i) = \frac{e^{-a\bar{x}} \sin\varphi_\pm(x_i) - \sin(\omega_\pm \pi \bar{x} + \varphi_\pm(x_i))}{\sqrt{\omega_\pm^2 \pi^2 + a^2}}, \tag{15}$$

in terms of a function

$$\varphi_\pm(x_i) = \omega_\pm \pi x_i - \phi_\pm, \tag{16}$$

and constants $\phi_\pm$ defined by

$$\tan\phi_\pm = \omega_\pm \pi / a, \qquad \phi_\pm \in (0, \tfrac{\pi}{2}). \tag{17}$$

More useful than the solutions themselves is the map through $S_+$ or $S_-$ between successive contact points with $S_0$. Let $P_\pm^a : \mathbb{R} \to \mathbb{R}$ be defined as

$$P_\pm^a(x_i) = x_i + \bar{x}_{i+1}, \tag{18}$$

with $\bar{x}_{i+1} = x_{i+1} - x_i$; then $x_{i+1}$ satisfies $x_{i+1} = P_\pm^a(x_i)$. Since $a > 0$, any trajectory will eventually hit $S_0$ in finite time, so there always exists a next intersection point $x_{i+1}$ following any $x_i$, and for a certain $y_\pm(\bar{x}, x_i)$ it is given by

$$\begin{aligned} \bar{x}_{i+1} &= \min_{\bar{x}} \left\{ \bar{x} \in \mathbb{R}^+;\ y_\pm(\bar{x}, x_i) = 0 \right\} \\ &= \min_{\bar{x}} \left\{ \bar{x} \in \mathbb{R}^+;\ h_\pm(\bar{x}, x_i) = 0 \right\}, \end{aligned} \tag{19}$$

in terms of a function

$$h_\pm(\bar{x}, x_i) = e^{-a\bar{x}} \sin\varphi_\pm(x_i) - \sin(\omega_\pm \pi \bar{x} + \varphi_\pm(x_i)). \tag{20}$$

Although $h_\pm(\bar{x}, x_i) = 0$ is a transcendental equation and explicit solutions cannot be computed, the zeros of these functions will be useful to bound such contact points. Let

$$h_\pm^0(\bar{x}, x_i) := \sin\varphi_\pm(x_i) - \sin(\omega_\pm \pi \bar{x} + \varphi_\pm(x_i)), \tag{21}$$

$$h_\pm^\infty(\bar{x}, x_i) := -\sin(\omega_\pm \pi \bar{x} + \varphi_\pm(x_i)). \tag{22}$$

Solving for $\bar{x}$, the zeroes of $h_\pm^0(\bar{x}, x_i)$ lie at

$$\bar{x} = \frac{2n}{\omega_\pm} \quad \text{or} \quad \frac{2n+1}{\omega_\pm} + \frac{2\phi_\pm}{\omega_\pm \pi} - 2x_i, \qquad n = 0, 1, 2 \ldots, \tag{23}$$

and the zeroes of $h_{\pm}^{\infty}(\bar{x}, x_i)$ lie at

$$\bar{x} = \frac{n}{\omega_{\pm}} - \frac{\varphi_{\pm}(x_i)}{\omega_{\pm}\pi} = \frac{n}{\omega_{\pm}} + \frac{\phi_{\pm}}{\omega_{\pm}\pi} - x_i, \quad n = 0, 1, 2 \ldots \tag{24}$$

Although we are interested only in the case $a > 0$, we note that for $a = 0$ the equation $h_{\pm}(\bar{x}, x_i) = 0$ is solvable, and implies $\phi_{\pm} = \frac{\pi}{2}$, so the map reduces to

$$P_{\pm}^{0}(x_i) = \tfrac{2}{\omega_{\pm}}(1 + \lfloor \omega_{\pm} x_i \rfloor) - x_i \tag{25}$$

where $\lfloor u \rfloor$ denotes the largest integer such that $\lfloor u \rfloor \leq u$.

## 3. Periodic solutions in the piecewise-smooth system

### *3.1. Linear switching*

Let us assume that the forcing is defined by (6a). The system (5) can then be re-written as

$$\dot{x} = 1, \tag{26a}$$

$$\dot{y} = -ay - [1 + (1 + \lambda)\cos \pi x] \sin \tfrac{\pi x}{2}, \tag{26b}$$

with $\lambda = \text{sign}(y)$ in $S_{\pm}$, and $\lambda \in (-1, 1)$ in $S_0$.

It follows from (11) and (26b) that sliding occurs in intervals on $S_0$ where $x$ can satisfy

$$[1 + (1 + \lambda)\cos \pi x] \sin \tfrac{\pi x}{2} = 0 \quad \text{for} \quad \lambda \in (-1, 1)\ .$$

There are isolated solution points when $\sin \frac{\pi x}{2} = 0$, i.e. at $x = 2n$ for $n \in \mathbb{N}$, but these do not give motion along $S_0$. Assuming $\sin \frac{\pi x}{2} \neq 0$, then $x$ must satisfy

$$-1 < \lambda = -1 - \sec \pi x < 1$$

hence $0 < -\sec \pi x < 2$, implying $\cos \pi x < -\frac{1}{2}$, so

$$x \in \left(\tfrac{2}{3} + 2n, \tfrac{4}{3} + 2n\right), \quad n \in \mathbb{N}\ .$$

Notice that the sliding manifolds $\Lambda^L$, defined in (11), correspond to the cases $n = 2k + 1$, $k \in \mathbb{N}$ in the above equation, which are *attracting*.

Making use of these sliding manifolds on $S_0$, and the function $P$ on $S_{\pm}$ from (18), periodic orbits are shown to exist with or without sliding in this system. Let us first start with non-sliding periodic solutions.

**Theorem 1.** *There exists $a_l \in \mathbb{R}^+$, $a_l \ll 1$, such that for all $a \in (0, a_l)$ system* (26) *has a non-sliding periodic solution, which is* 4*-periodic and locally asymptotically stable.* □

The proof of this theorem is given in Appendix A.1.

Numerical computations show that a solution of (A.3) in $\left(0, \frac{2}{3}\right)$ is given by $x_0 = 0.6357545163..$, and that, for example, the non-sliding periodic solution for $a = 0.01$ crosses $S_0$ at $x = 0.6261249968..$ (to 10 significant figures, simulated in Figure 3).

In turn, we can prove the existence of sliding periodic solutions for large values of $a$ by showing that a solution exiting the sliding interval $x \in \left(\frac{8}{3}, \frac{10}{3}\right)$ through its right hand side extremum, arrives in the next sliding interval, $x \in \left(\frac{20}{3}, \frac{22}{3}\right)$ after several crossings of $S_0$.

**Theorem 2.** *There exists $a_h \in \mathbb{R}^+$, $a_h \gg 1$, such that for all $a \in (a_h, +\infty)$, system* (26) *has a sliding* 4*-periodic solution. Moreover, for every $a \in (a_h, +\infty)$ there exists $\nu(a) \in \mathbb{R}^+$ such that solutions $y(x, x_i)$ of* (26)*, with $x_i \in \left(\frac{8}{3}, \frac{10}{3}\right) \cup \left(\frac{10}{3}, \frac{10}{3} + \nu(a)\right)$, converge in finite time to the periodic solution $y\left(x, \frac{10}{3}\right)$.*

The proof of this theorem is given in Appendix A.2.

Numerical simulations appear to show that sliding periodic solutions exist for a wide range of values of $a$, failing to appear only for $a \to 0$. Some examples are simulated in Figure 4.

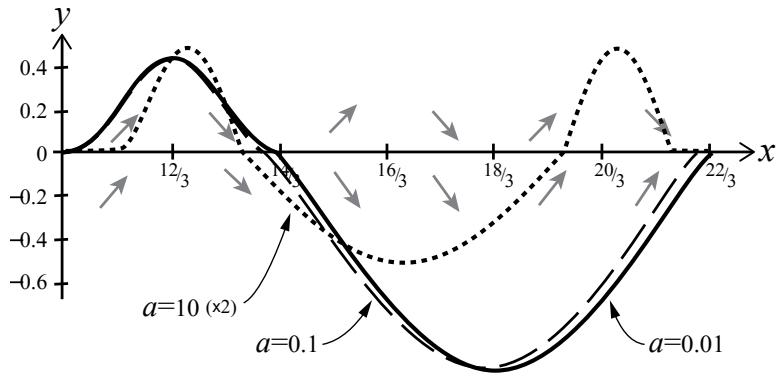


Figure 4: Period 4 orbits of the linear switching system, showing: a non-sliding orbit for $a = 0.01$ (full curve), an orbit with a small segment of sliding for $a = 0.1$ (dashed curve), and a sliding orbit for $a = 10$ (dotted curve, vertical scale multiplied by 1/2 for clarity).

*3.2. Nonlinear switching*

Let us assume that the forcing is defined by (6b). Then (5) can be written as

$$\dot{x} = 1, \tag{27a}$$
$$\dot{y} = -ay - \sin\left[\pi x \left(1 + \tfrac{1}{2}\lambda\right)\right], \tag{27b}$$

with $\lambda = \mathrm{sign}(y)$ in $S_{\pm}$, and $\lambda \in (-1, 1)$ in $S_0$.

It follows from (13) and (27b) that the sliding time intervals are defined by

$$\sin\left(\pi x \left[1 + \tfrac{1}{2}\lambda\right]\right) = 0, \quad \lambda \in (-1, 1) < 1 \, .$$

Therefore $-1 < \lambda = 2\left(\frac{n}{x} - 1\right) < 1$, hence

$$x \in \left(\tfrac{2n}{3}, 2n\right) \quad \text{for} \quad n \in \mathbb{N} \setminus \{0\} \, .$$

From the above formula, we obtain the sliding sets $\Lambda_n^N$ and $\Lambda^N$, introduced in (12), which correspond to take $n = 2k$, $k \geq 1$.

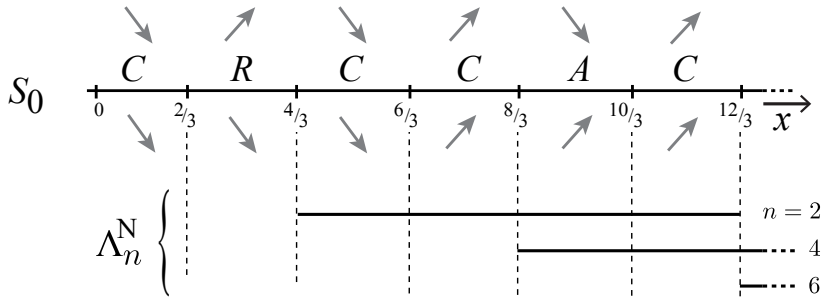


Figure 5: The nonlinear switching system has sliding manifolds (branches of $\Lambda^N$) on $S_0$, represented here to show how they overlap increasingly with larger $x$.

The sliding manifolds for $n = 2, 4, 6$ are depicted in Figure 5. It turns out that sliding may take place on $x \in (\frac{4n}{3}, 4n)$, $n \geq 1$, irrespective of the directions of the vector field outside the switching manifold, i.e. not only through regions of attractive sliding, but also of repelling sliding and crossing. For $x > \frac{4}{3}$ the sliding manifolds overlap as illustrated in Figure 5, and a regularization is needed to disclose on which manifold(s) a trajectory will evolve after hitting the switching manifold, and whether they can ever leave the switching manifold.

The sliding manifolds defined in (12) depend on $n$, such that a trajectory evolving on a specific manifold may slide for a maximum distance in $x$ of

$$\Delta x(n) = 4n - \tfrac{4n}{3} = \tfrac{8n}{3} \ .$$

This reveals a sort of *ageing* in the system, as the 'later' in $x$ a trajectory undergoes sliding motion, the 'longer' sliding might persist. Such a situation is not found in the linear case, where all the sliding intervals have a constant length of $\frac{2}{3}$ (recall (11)).

Let us now analyze sliding and non-sliding periodic solutions. In contrast to the linear case, the overlapping of sliding manifolds prevents the existence of non-sliding periodic solutions, as the following results show.

**Theorem 3.** *System* (27) *does not have non-sliding periodic solutions.*

The proof of this theorem is given in Appendix A.3.

As regards periodic solutions, from the direction of the vector fields in $S_\pm$ (see Figure 2) we can discern that a sliding solution on $\Lambda^N$ must have

$$\text{entered from } S_+ \text{ if } x \in \left(\tfrac{4n-2}{3}, \tfrac{4n+2}{3}\right), \text{ or} \tag{28a}$$

$$\text{entered from } S_- \text{ if } x \in (4n-2, 4n), \tag{28b}$$

with $x$ denoting the time of entry.

**Theorem 4.** *For all $a \in \mathbb{R}^+$, there exists $x_a \in (2,4)$ such that system* (27) *has a unique sliding 4-periodic solution, $y_d(x)$, which lies in $\overline{S}_-$ and satisfies*

$$y_d(x) < 0, \quad x \in (4n, 4n + x_a)\,, \tag{29}$$

$$y_d(x) = 0, \quad x \in \{0\} \cup [4n + x_a, 4(n+1)]\,, \quad n \in \mathbb{N}. \tag{30}$$

The proof of this theorem can be found in Appendix A.4.

**Theorem 5.** *For all $a \in \mathbb{R}^+$, all solutions starting in $S_+$ have their evolutions constrained in $\overline{S}_-$ for all $x$ large enough. Moreover, they overlap with the periodic solution described in Theorem 4 for $x \geq 4n$, with $n \in \mathbb{N}$.*

The proof of this Theorem can be found in Appendix A.5.

Figure 6 illustrates the solutions described in Theorem 4 and Theorem 5.

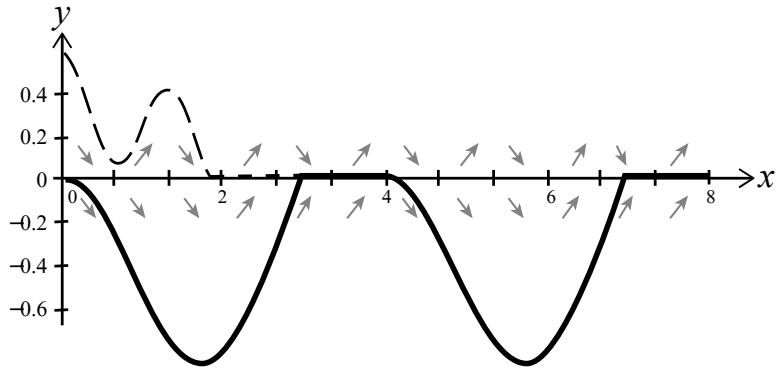


Figure 6: Orbits of the nonlinear switching system, showing: a period 4 sliding solution (full curve, as described by Theorem 4) and a solution attracted onto it in finite time (dashed curve, as described by Theorem 5). All simulated for $a = 0.5$.

## 4. Dynamics of a regularized system

The dynamics of our two switching systems is only partially resolved by the analysis in Section 3.1 and Section 3.2, because, although the two systems are identical outside $y = 0$, they have different dynamics on $y = 0$. Moreover there are numerous sliding manifolds in the nonlinear system, each resulting in sliding dynamics that exists for different but overlapping intervals in $x$, with increasing numbers of manifolds overlapping as $x$ increases. To resolve which of these motions is possible in the system, and how they connect to the dynamics outside $y = 0$, requires us to regularize the discontinuity.

It has been shown that different regularizations can lead to different dynamics [2, 3, 15, 16], and which is most appropriate depends on the application or the question being posed. Our aim here is to show that the differences between the linear and nonlinear switching systems shown in Section 3.1 and Section 3.2, persist under the *same* regularization. For this we use the Sotomayor-Teixeira regularization [27], which has been extensively studied, and has the advantage of resulting in a system that is not only smoothly differentiable, allowing us study it using geometric singular perturbation methods, but is also identical to the original discontinuous system for all $|y| > \varepsilon$ for some small $\varepsilon$.

The regularization involves replacing the switching manifold by a switching layer of width order $\epsilon > 0$, namely

$$S_0^\epsilon := \left\{(x, y) \in \mathbb{R}^2 \ : \ -\epsilon < y < \epsilon\right\} \ . \tag{31}$$

Here we shall do this in a manner that yields a smooth system, replacing the switching multiplier $\lambda = \text{sign}(y)$ by a transition function $\psi\left(\frac{y}{\epsilon}\right)$ satisfying

$$\psi'\left(\frac{y}{\epsilon}\right) > 0 \quad \text{for} \quad |y| < \epsilon \,, \tag{32a}$$

$$\psi\left(\frac{y}{\epsilon}\right) = \text{sign}(y) \quad \text{for} \quad |y| \geq \epsilon \,, \tag{32b}$$

$$\text{sign}\left(\psi''\left(\frac{y}{\epsilon}\right)\right) = -\text{sign}(y) \quad \text{for} \quad |y| = \epsilon \,, \tag{32c}$$

from which it follows that $|\psi(\frac{y}{\epsilon})| < 1$ for $|y| < \epsilon$ and $\psi'(\frac{y}{\epsilon}) = 0$ for $|y| \geq \epsilon$. We will not consider analytic transition functions, like $\tanh(z)$ or $\frac{2}{\pi}\arctan(z)$, because they would perturb the vector fields globally, and in standard regularization approaches (especially following [27]) non-analytic functions are preferred such that $\psi = \pm 1$ outside the transition layer.

The half-planes corresponding to $S_\pm$, defined in (7) for the discontinuous system, become

$$S_\pm^\epsilon := \left\{(x, y) \in \mathbb{R}^2 \ : \ \pm y \geq \epsilon\right\}. \tag{33}$$

The regularization of the system (5) is simply obtained by substituting $\psi(y/\varepsilon)$ in place of $\lambda$. In terms of a fast variable $v = y/\epsilon$ this becomes

$$\dot{x} = 1 \,, \tag{34a}$$

$$\epsilon\dot{v} = -a\epsilon v - f_i\left(x, \psi\left(v\right)\right) \,, \tag{34b}$$

where $f_i$ and $f_L$ are the functions defined in (6).

Re-scaling to a fast time variable $\tau = t/\epsilon$ yields the fast subsystem

$$x' = \epsilon \,, \tag{35a}$$

$$v' = -a\epsilon v + f_i\left(x, \psi\left(v\right)\right) \,, \tag{35b}$$

denoting the time derivative as $x' \equiv \varepsilon\dot{x}$. The limit $\epsilon \to 0$ results in

$$x' = 0 \,, \tag{36a}$$

$$v' = f_i\left(x, \psi\left(v\right)\right) \,, \tag{36b}$$

which provides the fast dynamics along the $v$ direction, parameterized by $x$, outside the slow critical manifold

$$\Lambda_0^i = \left\{(x, v) : \ f_i\left(x, \psi\left(v\right)\right) = 0, \ |v| < 1\right\} \,, \tag{37}$$

which is the equivalent of the sliding manifold $\Lambda^i$ of the discontinuous system defined in (11), where again $i$ labels the linear or nonlinear model as in (6);

the subscript '0' denotes that this is assocated with the $\varepsilon = 0$ system i.e. the *critical manifold* of (34), while the *slow manifolds* for $\varepsilon > 0$ will be denoted $\Lambda^i_\varepsilon$. The critical manifold is an invariant of the limiting system (i.e. with $\epsilon = 0$) wherever it is normally hyperbolic, i.e. where

$$\frac{\partial}{\partial v} f_i\left(x, \psi\left(v\right)\right) \neq 0, \tag{38}$$

and the positivity (or negativity) of this partial derivative indicates that $\Lambda^r_0$ is unstable (or stable).

Notice also that the analogues of $S^\epsilon_0$ and $S^\epsilon_\pm$ in the $(x, v)$ plane are

$$V_0 := \left\{(x, v) \in \mathbb{R}^2 \ : \ |v| < 1\right\}, \tag{39a}$$

$$V_\pm := \left\{(x, v) \in \mathbb{R}^2 \ : \ \pm v \geq 1\right\}. \tag{39b}$$

(These are independent of $\varepsilon$ because it has been scaled out by the $v$ coordinate).

In turn, for $\epsilon \neq 0$ the fold points on $v = \pm 1$ lie at $O(\epsilon)$ distance from those of the limiting ($\varepsilon = 0$) system, namely,

$$x^\pm_{4n} := \frac{4n}{2 \pm 1}, \qquad x^\pm_{4n+2} := \frac{4n+2}{2 \pm 1}. \tag{40}$$

Indeed, it follows from (34b) that, at the fold points, $x^\pm_{\epsilon,k}$, one has

$$-a\epsilon\left(\pm 1\right) - \sin\left(\pi\omega_\pm x^\pm_{\epsilon,k}\right) = 0, \tag{41}$$

where it is assumed that $a\epsilon \ll 1$, then

$$x^\pm_{\epsilon,4n} := x^\pm_{4n} \mp \frac{1}{\pi\omega_\pm} \arcsin(a\epsilon), \tag{42a}$$

$$x^\pm_{\epsilon,4n+2} := x^\pm_{4n+2} \pm \frac{1}{\pi\omega_\pm} \arcsin(a\epsilon). \tag{42b}$$

This is illustrated in Figure 7.

We show below that the qualitative dynamics of the linear switching system (using $f_L$ from (6a)) is preserved under regularization, including both sliding and non sliding periodic solutions. The qualitative dynamics of the nonlinear switching system (using $f_N$ from (6b)) is also preserved, but instead of an exact period 4 solution, there exists an orbit asymptotically approaching period 4, with its segment in the layer $V_0$ deforming slightly with increasing $x$. Moreover we are able to show that under regularization:

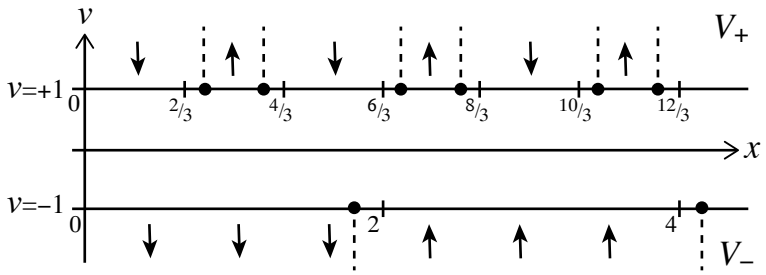


Figure 7: Fold points (bold circles) and direction of the vector field for the regularized case.

i) ageing persists, such that branches of the sliding manifold not only increase in length with $x$ but do not overlap, so the system is not periodic inside the layer $V_0$ and fully periodic orbits are impossible;

ii) for $x \to +\infty$ most of solutions evolve towards a *periodic object* (see Definition 7) located in $V_-$ which, for $\epsilon \to 0$, becomes the period 4 orbit of the discontinuous system described in Theorem 4 (similar to the behaviour illustrated by the full curve and dashed curve in Figure 6 but without periodicity).

As in previous sections we take the linear and nonlinear systems in turn.

*4.1. Regularization of the linear switching system*

Take the system (34) using the forcing $f_L$ defined in (6a) (or equivalently substitute $\lambda \mapsto \psi(y/\varepsilon)$ into (26)). We obtain

$$\dot{x} = 1, \tag{43a}$$

$$\epsilon \dot{v} = -a\epsilon v - [1 + (1 + \psi(v)) \cos \pi x] \sin \tfrac{\pi x}{2}. \tag{43b}$$

It follows from (37) that the critical manifolds are defined by

$$[1 + (1 + \psi(v)) \cos \pi x] \sin \tfrac{\pi x}{2} = 0, \quad |v| < 1 \, . \tag{44}$$

Therefore $-1 < \lambda = 2\left(\frac{n}{x} - 1\right) < 1$, implying $x \in \left(\frac{2n}{3}, 2n\right)$ for $n \in \mathbb{N} \setminus \{0\}$. However, by (32) the function $\psi$ satisfies $|\psi(v)| < 1$, therefore

$$-1 < \psi(v) = -1 - \sec \pi x < 1 \, , \tag{45}$$

hence $0 < -\frac{1}{\cos \pi x} < 2$, implying $\cos \pi x < -\frac{1}{2}$ and therefore

$$x \in \left(\tfrac{2}{3} + 2n, \tfrac{4}{3} + 2n\right), \quad n \in \mathbb{N} \, . \tag{46}$$

As in defining $\Lambda^L$ we may exclude the point where $\sin \frac{\pi x}{2} = 0$, hence where $x = 2n$ for $n \in \mathbb{N}$. Following (38), $\Lambda_0^L$ is invariant where

$$0 \neq \frac{\partial}{\partial v} f\left(x, \psi\left(v\right)\right) = -\psi'\left(v\right) \cos \pi x \sin \tfrac{\pi x}{2} \ , \tag{47}$$

and since $\psi'\left(v\right) > 0$ for all $v \in (-1, 1)$ by (32a), the result follows.

Therefore, the critical manifolds of (43) (in the limit $\epsilon = 0$) are given by

$$\Lambda_0^L := \left\{(x, v) \in V_0 \ : \ \psi\left(v\right) = -1 - \sec \pi x, \ x \in \left(\tfrac{2}{3} + 2n, \tfrac{4}{3} + 2n\right), \ n \in \mathbb{N}\right\}. \tag{48}$$

Finally, from the sign of $\frac{\partial}{\partial v} f\left(x, \psi\left(v\right)\right)$ in (47) we have that

$$\text{on} \ \ x \in \left(\tfrac{2}{3} + 4n, \tfrac{4}{3} + 4n\right) \ \ \Lambda_0^L \ \text{ is repelling}, \tag{49a}$$

$$\text{on} \ \ x \in \left(\tfrac{8}{3} + 4n, \tfrac{10}{3} + 4n\right) \ \ \Lambda_0^L \ \text{ is attracting}, \tag{49b}$$

with $n \in \mathbb{N}$. These $x$-intervals match those obtained for $\Lambda^L$ in the discontinuous linear system in Section 3.1 as illustrated in Figure 2.

As an example, the critical manifolds corresponding to the $x$-intervals defined in (49) for $n = 1$, letting

$$\psi\left(v\right) = \begin{cases} -1 & v < -1 \ , \\ \frac{1}{2} v \left(3 - v^2\right) & -1 \leq v \leq 1 \ , \\ 1 & v > 1 \ , \end{cases} \tag{50}$$

are depicted in Figure 8.

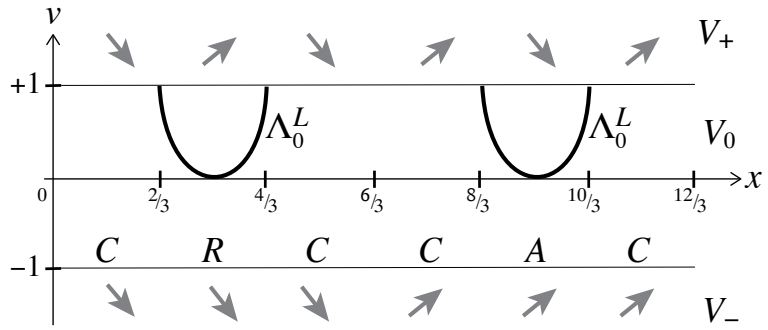


Figure 8: Linear regularization, showing the switching layer $V_0$ and the sliding manifolds $\Lambda_0^L$ inside it, with a repelling branch (left) and attracting branch (right). Corresponding labels for regions of crossing and sliding from Figure 2 are shown, with the directions of the fields in $V_\pm$.

The persistence of the non-sliding and sliding periodic solutions are established below by analogous results to those of Theorem 1 and Theorem 2.

**Theorem 6.** *For all $a, \epsilon \in \mathbb{R}$ such that $0 < a \ll 1$ and $0 < \epsilon \ll 1$, system (43) has a non-sliding periodic solution, which is 4-periodic and locally asymptotically stable.*

The proof of this theorem is given in Appendix A.6.

**Theorem 7.** *For all $a, \epsilon > 0$ such that $a \gg 1$ and $\epsilon \ll 1$, system (43) has a sliding 4-periodic solution. Such a solution is locally asymptotically stable, with Lipschitz constant exponentially small in $\epsilon$.*

The proof of this theorem is given in Appendix A.7.

In Figure 9 we simulate a 4-periodic non-sliding solution for $a = 0.01$, and a 4-periodic sliding periodic solution for $a = 2$. The two lower panels show a magnification of the trajectories passing through the switching layer. Notice the equivalence with the solutions plotted in Figure 3 from the discontinuous system.

*4.2. Regularization of the nonlinear switching system*

Take the system (34) using the forcing $f_N$ defined in (6b) (or equivalently substitute $\lambda \mapsto \psi(y/\varepsilon)$ into (27)). We obtain

$$\dot{x} = 1, \tag{51a}$$

$$\epsilon \dot{v} = -a\epsilon v - \sin\left(\pi x \left[1 + \tfrac{1}{2}\psi\left(v\right)\right]\right). \tag{51b}$$

It is straightforward from (37) that the critical manifolds are defined by

$$\sin\left(\pi x \left[1 + \tfrac{1}{2}\psi\left(v\right)\right]\right) = 0, \quad |v| < 1\,. \tag{52}$$

The result follows proceeding as in the linear case, noting the manifolds are invariant everywhere, since

$$\begin{aligned} \frac{\partial}{\partial v} f_N\left(x, \psi\left(v\right)\right) &= -\tfrac{\pi x}{2}\psi'\left(v\right)\cos\left(\pi x \left[1 + \tfrac{1}{2}\psi\left(v\right)\right]\right) \\ &= -\tfrac{\pi x}{2}\psi'\left(v\right)\cos n\pi = \tfrac{(-1)^{n+1}\pi x}{2}\psi'\left(v\right) \neq 0. \end{aligned} \tag{53}$$

Therefore, the critical manifolds of (51) (in the limit $\epsilon = 0$) are given by

$$\left\{(x, v) \in V_0 :\ \psi\left(v\right) = 2\left(\tfrac{n}{x} - 1\right),\ x \in \left(\tfrac{2n}{3}, 2n\right),\ n \in \mathbb{N} \setminus \{0\}\right\}. \tag{54}$$

Examples of the critical manifolds corresponding to $n = 1, 2 \ldots, 10$, are shown in Figure 10, again using (50).

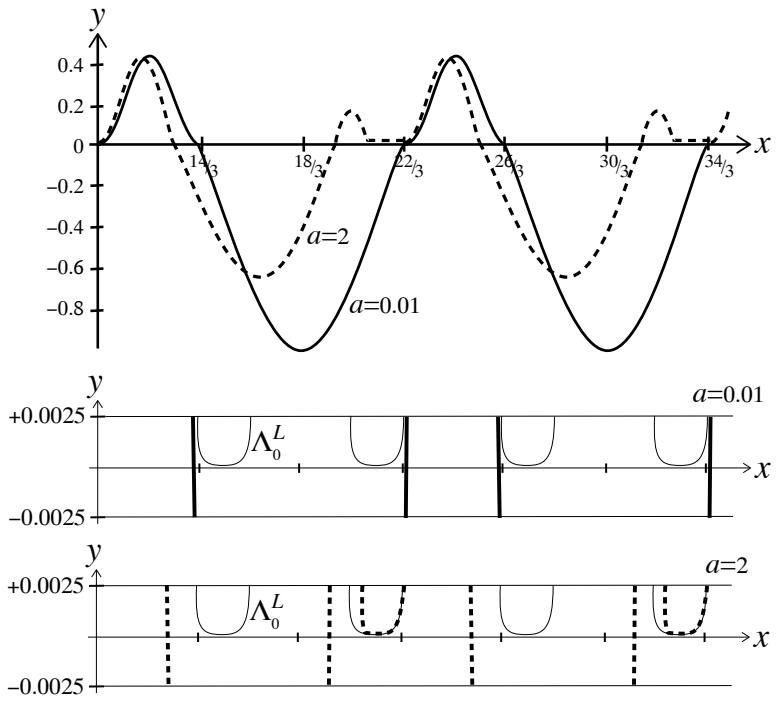


Figure 9: Linear regularization, showing a non-sliding period 4 solution (full curve) for $a = 0.01$ passing through the point $(x_0, y_0) = (0, 0.42)$, and a sliding period 4 solution (dotted curve) for $a = 2$ passing through the point $(x_0, v_0) = \left(-\frac{2}{3}, 0.0019\right)$; both simulated from (43) with $\epsilon = 0.0025$. The lower panels are magnifications of the switching layer, showing the solution passing through the layer, and in the latter case evolving close to the critical manifold $\Lambda_0^L$.

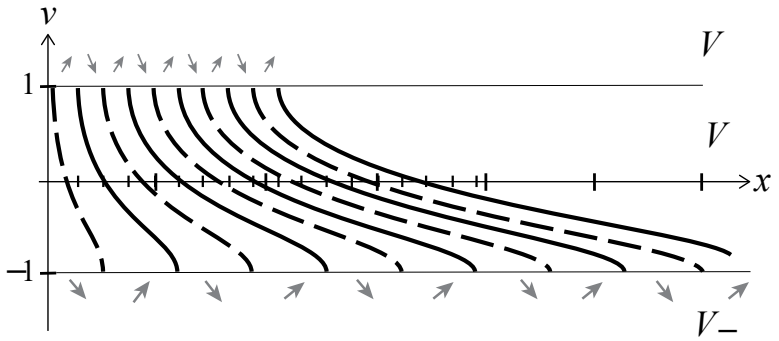


Figure 10: Nonlinear regularization, showing the switching layer $V_0$ and the critical manifolds inside it, with repelling branches (dashed) and attracting branches (full), for $n = 1, 2 \ldots 10$. Arrows indicate the direction of the vector fields in $S_\pm$.

Taking into account the sets $\Lambda_n^N$ introduced in (12) and (53), the stable critical manifolds will be denoted by

$$\Lambda_{0n}^N := \left\{ (x,v) \in V_0 : \ \psi(v) = 2\left(\frac{2n}{x} - 1\right), \ x \in \left(\frac{4n}{3}, 4n\right) \right\}. \tag{55}$$

Notice that, recalling (12), (40) and (42), $\left(\frac{4n}{3}, 4n\right) = \left(x_{4n}^+, x_{4n}^-\right) = \Lambda_n^N$.

We can then prove the following theorem.

**Theorem 8.** *Let $(x(t), v(t))$ be a solution of system (51), with $\epsilon$ small enough. The following are true.*

1. *Ageing phenomenon: for all $(x_0, v_0)$ with $x_0 > 1$ and $v_0 \geq 1$, except a set of arbitrarily small measure in any compact set of $V_+$, if $(x(0), v(0)) = (x_0, v_0)$, then $(x(t), v(t))$ satisfies $|v(t)| < 1$, for $t$ in an interval of length larger than $2x_0 - 2$, that is, when $\epsilon \to 0$ the corresponding solution of the discontinuous system has a sliding part of length larger that $2x_0 - 2$.*
2. *$\omega$-limit of solutions: as $x \to +\infty$, all trajectories of system (51) with $|v_0| \geq 1$, except a set of arbitrarily small measure in any compact set of $V_+ \cup V_-$, tend to a 4-periodic function $v_r(x)$, whose graph is included in $V_-$ which, when $\epsilon \to 0$ tends to the periodic orbit obtained in Theorem 7.*

See Definition 7 for the precise definition of $v_r(x)$. The proof of this (see Appendix A.8) follows the steps:

1. Fix $\delta > 0$. Then, for any $\epsilon > 0$ small enough, all solutions with $v(0) > 1$, except a set of *small* measure, intersect transversally $v = 1$ in finite time at a point $(x, 1)$ with $x \in (x_{\epsilon,4n}^+, \frac{4n+2}{3} - 2\delta)$, $n \geq 1$, where, recalling (42), $x_{\epsilon,4n}^+ = \frac{4n}{3} - \frac{2}{3\pi}\arcsin(a\epsilon)$. See Figure 11.
2. In the region $V_0$, the dynamics is governed by the stable critical manifolds, $\Lambda_{0n}^N$, which are enveloped within the manifolds

$$\Lambda_{\pm\delta n}^N := \left\{ (x,v) \in \mathbb{R}^2 : \psi(v) = \frac{4n \pm 3\delta}{x} - 2, x \in \left[\tfrac{4n}{3} \pm \delta, 4n \pm 3\delta\right] \right\}, \tag{56}$$

   where $\delta \in \mathbb{R}^+$ is such that

$$1 \gg \delta > x_{4n}^+ - x_{\epsilon,4n}^+ = \tfrac{2}{3\pi}\arcsin(a\epsilon). \tag{57}$$

   We will see that close to $\Lambda_{0n}^N$ the system possesses stable Fenichel manifolds confined by the curves $\Lambda_{\pm\delta n}^N$, see Figure 12.

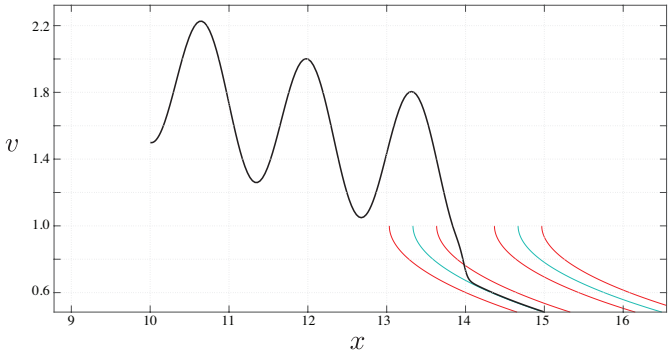


Figure 11: A solution (black curve) enters $V_0$ after some positive time, also showing the stable critical manifolds (blue curves) and the curves $\Lambda^N_{\pm\delta n}$ (red curves).

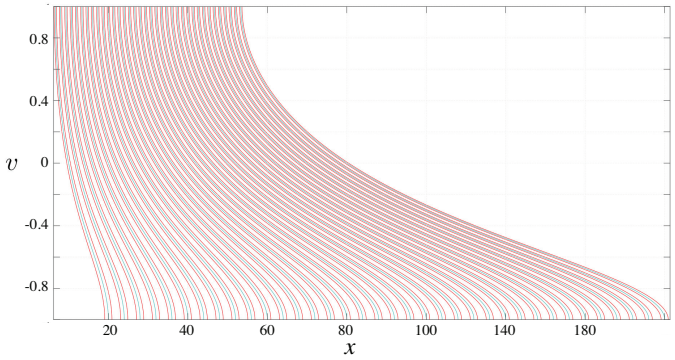


Figure 12: The stable critical manifolds (blue curves), and the curves $\Lambda^N_{\pm\delta n}$ (red curves).

3. All solutions with initial conditions $(x, 1)$ with $x \in (x^+_{\epsilon,4n}, (4n+2)/3 - 2\delta)$, $n \geq 1$ intersect $x = (4n+2)/3 - \delta$, with $v$ such that $(x, v)$ lies between the curves $\Lambda^N_{\pm\delta n}$. See Figure 13.
4. In the region

$$\mathcal{V}_{2\delta n} := \left\{ (x,v) \in \mathbb{R}^2 : \; x \in \left[ \frac{4n}{3} + 2\delta, 4n - 6\delta \right] \; \wedge \; |v| \leq 1 \right.$$
$$\left. \wedge \; \frac{4n-3\delta}{x} - 2 \leq \psi(v) \leq \frac{4n+3\delta}{x} - 2 \right\}, \tag{58}$$

there is a stable Fenichel manifold at a distance $\mathcal{O}(\epsilon/n)$ of the critical manifold $\Lambda^N_{0n}$. We remark that although the length of the region increases with $n$ while $\epsilon$ remains fixed, the distance between the Fenichel and critical manifolds decreases with $n$. This fact allows us to overcome the lack of compactness in $n$. In particular, at the exit part of

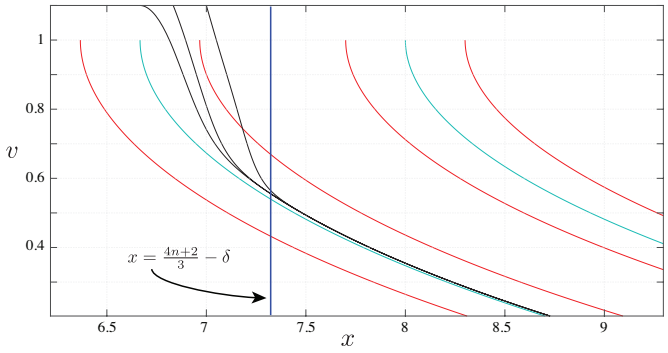


Figure 13: Solutions intersect $x = \frac{4n+2}{3} - \delta$ between the curves $\Lambda^N_{\pm\delta n}$ (red). Stable critical manifolds are also shown (blue curves). Plotted for $n = 5$, $\delta = 0.3$, $\epsilon = 0.5$.

$\mathcal{V}_{2\delta n}$, we only need to follow the Fenichel manifold, since all solutions starting in $(x, 1)$ with $x \in (x^+_{\epsilon,4n}, (4n+2)/3 - 2\delta)$, $n \geq 1$, have been exponentially trapped by a factor $\mathcal{O}(e^{-n/\epsilon})$ by the Fenichel manifold. See Figure 14.

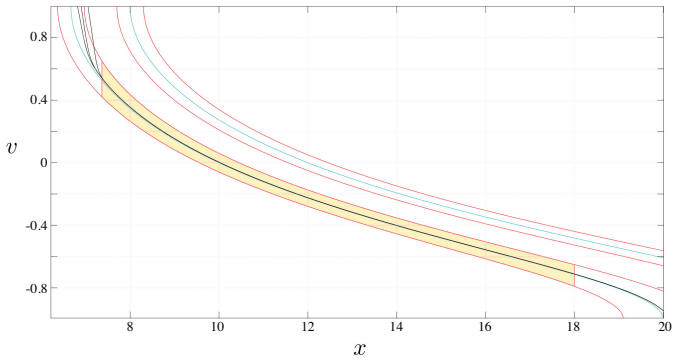


Figure 14: In the region $\mathcal{V}_{2\delta n}$ (yellow shaded region), solutions are exponentially close to the Fenichel manifold, which is $\mathcal{O}(\epsilon/n)$ close to the critical manifold. Stable critical manifolds and curves $\Lambda^N_{\pm\delta n}$ are shown in blue and red as in Figure 11 onwards.

5. When leaving the region $\mathcal{V}_{2\delta n}$, the Fenichel manifold starts losing hyperbolicity. In order to study its continuation, the system has to be approximated by a Riccati equation. Blow-up methods or asymptotic matching theory imply that the Fenichel manifold reaches $v = -1$ at a point, $\bar{x}^-_{\epsilon,4n}$, which is within $\mathcal{O}(\epsilon^{2/3}/n^{1/3})$ to the right of $x^-_{\epsilon,4n} = 4n + 2\arcsin(a\epsilon)/\pi$, the fold point (recall (42)). See Figure 15.
6. Once the Fenichel manifold enters $V_-$ by $\bar{x}^-_{\epsilon,4n}$, at the right of the

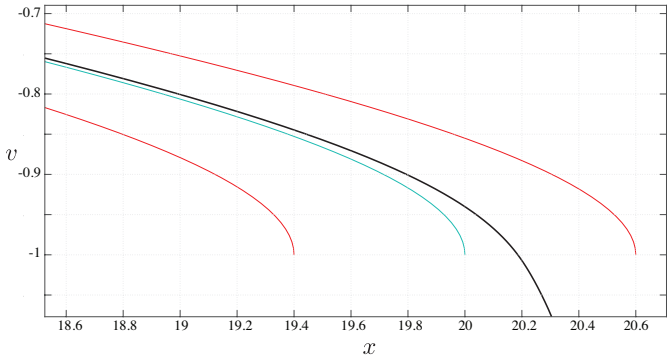


Figure 15: The Fenichel manifold (black curve), follows the Riccati equation when leaving the regularization zone $V_0$ at a point, $\bar{x}^-_{\epsilon,4n}$, which within $\mathcal{O}(\epsilon^{1/3}/n^{2/3})$ to the right of $x^-_{\epsilon,4n} = 4n + 2\arcsin(a\epsilon)/\pi$. Plotted for $a = 10^{-2}$, $\epsilon = 0.5$, $n = 5$. Stable critical manifolds and curves $\Lambda^N_{\pm\delta n}$ are shown in blue and red as in Figure 11 onwards.

fold point $x^-_{\epsilon,4n}$, close to $4n$, it is driven by the lower linear flow and bounded by below by the solution starting at $x^-_{\epsilon,4n}$. The latter hits $v = -1$ at a point within the next attracting interval, $\left(x^-_{\epsilon,4n+2}, x^-_{\epsilon,4n+4}\right)$, at $\mathcal{O}(\sqrt{a} + \varepsilon)$ to the left of $x^-_{4n+4} = 4n + 4$ (recall (40)), and so does the former at a maximum distance of $\mathcal{O}(\epsilon^{2/3}/n^{1/3})$. Then, both solutions enter $V_0$ and evolve therein upper bounded by the next (stable) Fenichel manifold, associated to $x^-_{4n+4}$, until they exit again into $V_-$ between its exiting point, $\bar{x}^-_{\epsilon,4n+4}$, and the next fold point close to $x^-_{4n+4}$, i.e. $x^-_{\epsilon,4n+4}$. See Figure 16.

7. The previous step is repeated. Due to the choice of our regularization function, the maximum height of the continuation of the Fenichel manifold close to $x^-_{4n}$ is $-1+\mathcal{O}(n^{-1/2})$. In turn, the length of the parts of the solution above $v = -1$ tends to a constant depending on $a, \epsilon$.

## 5. Conclusions

In Section 3.1 we showed that the linear switching system has a period 4 orbit, which is a crossing orbit for $a < a_l \ll 1$ and involves sliding for $a > a_h \gg 1$. We expect that this orbit exists for all $a$ (i.e. also for $a \geq a_l$ but not large), presumably undergoing a grazing-sliding bifurcation at some value in the range $a_l < a < a_h$. In the nonlinear system we showed that there exists a period 4 sliding solution for all $a$. The forms of the periodic orbits in the linear and nonlinear systems bare little relation to each other.

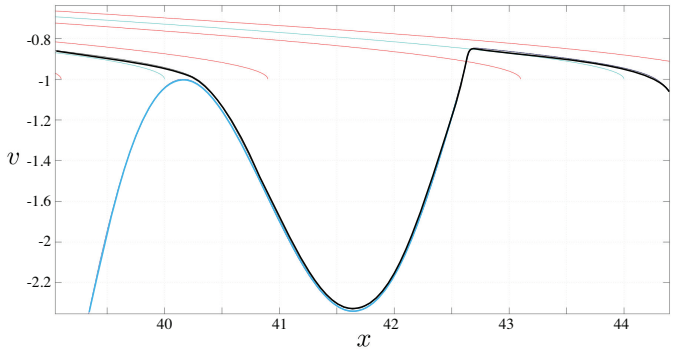


Figure 16: A solution (blue curve) starting at the fold point $x^-_{\epsilon,4n}$, close to $x^-_{4n}$, with $n = 10$. Note the flat region of the solution, of length $\mathcal{O}(\sqrt{a} + \varepsilon)$, lying close to the Fenichel manifold (black curve). Stable critical manifolds and curves $\Lambda^N_{\pm\delta n}$ are shown in blue and red as in Figure 11 onwards.

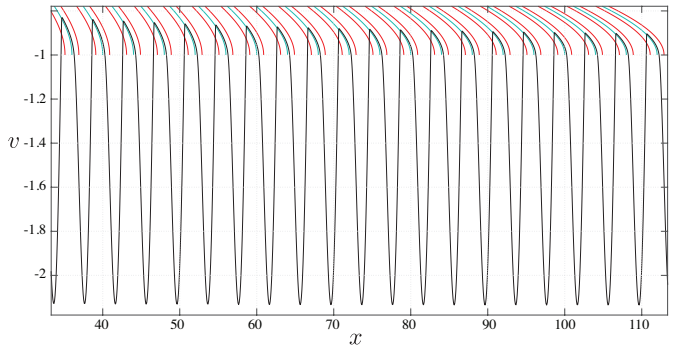


Figure 17: A solution whose highest point in $v$ can be seen (in the region $v > -1$)) decreasing with $n$. In the process, the length of the parts of the solution above $v = -1$ tends to a constant. Stable critical manifolds and curves $\Lambda^N_{\pm\delta n}$ are shown in blue and red as in Figure 11 onwards.

When the discontinuity was regularized the periodicity of the linear system persisted, while the nonlinear system tended towards a periodic orbit which itself was no longer an exact solution of the system. The analysis of the regularized nonlinear system is non-trivial because its slow manifolds become more crowded as time increases, despite which we have shown that sliding behaviour persists.

In the context of the resistor-inductor circuit in Figure 1 these results manifest as the current dynamics in cases where the controller can be modelled as switching linearly or non-linearly between frequency states. In the

linear case the circuit finds a stable oscillation, in the nonlinear case it ages until it becomes constrained to lower frequency state and the switching manifold. Experiments to observe such behaviour would certainly be of future interest, in electronic controllers or in other possible applications, with the focus being on distinguishing the linear-versus-nonlinear models of switching and the phenomenon of ageing.

Looking forward towards study of the original motivating system (1), we expect that the distinctions between linear and nonlinear switching arise very similarly to the relatively simple dynamics of the first order oscillator studied here. The added complexity of the second order oscillator lies mainly in the added dimension creating much richer sliding dynamics: whereas in the first order oscillator the sliding manifolds act merely as a barrier over long times, in the second order oscillator the ageing sliding manifolds bring to life a sequence of changing behaviours. Our preliminary investigations show first that lengthier segments of sliding are seen, similar to the first order oscillator here, followed later (for larger $t$) by relaxation oscillations and mixed-mode oscillations. These remain to be studied in detail, but with the first order system we have singled out the most important element that the example in [15] was conceived to show, namely the importance of linear versus nonlinear terms in models of switching, the different dynamics they create, and their persistence under regularization.

## Appendix A. Proof of main results

*Appendix A.1. Proof of Theorem 1*

Using the functions $P^a_\pm$ from (18), let us define

$$P(x,a) := \left(P^a_+ \circ P^a_-\right)(x)\,, \tag{A.1}$$

and also define intervals $I_- := \left(0, \frac{2}{3}\right)$ and $I_+ := \left(\frac{10}{3}, 4\right)$.

**Lemma 9.** *There exists $a_l \in \mathbb{R}^+$, $a_l \ll 1$, such that the roots of*

$$\Delta(x,a) := P(x,a) - (x+4) = 0 \tag{A.2}$$

*define a function $x = x(a)$ for all $a \in (0, a_l)$, which satisfies $x(0) = x_0$, with $x_0$ in $I_-$ being a solution of*

$$\tfrac{32}{9\pi} + \tfrac{2x_0}{3}\cot\frac{3\pi x_0}{2} + (4-2x_0)\cot\frac{\pi x_0}{2} = 0\,. \tag{A.3}$$

*Proof.* The mean value theorem implies that

$$\Delta(x,a) - \Delta(x,0) = (a-0)\frac{\partial \Delta}{\partial a}\left(x, \xi(a)\right) \ , \quad 0 < \xi(a) < a \ . \tag{A.4}$$

However, as it follows immediately using (25) that $\Delta(x,0) = P(x,0) - (x+4) = 0$, for all $x \in I_-$, the equation (A.4) implies

$$\Delta(x,a) = a\frac{\partial P}{\partial a}\left(x, \xi(a)\right), \quad 0 < \xi(a) < a. \tag{A.5}$$

Now, by the implicit function theorem, if there exists $x_0 \in I_-$ such that

$$\frac{\partial P}{\partial a}\left(x_0, 0\right) \ = \ 0 \ \neq \ \frac{\partial^2 P}{\partial x \partial a}\left(x_0, 0\right) \ , \tag{A.6}$$

then there exists $a_l \in \mathbb{R}^+$, $a_l \ll 1$, such that $\Delta(x,a) = 0$ defines a function $x = x(a)$ in $(0, a_l)$ satisfying $x(0) = x_0$ and with $\frac{\partial P}{\partial a}\left(x(a), \xi(a)\right) = 0$. Taking into account (20) and (16), $\frac{\partial P}{\partial a}\left(x_0, 0\right)$ in (A.6) is to be obtained from

$$h_-\left(P_-^a(x) - x, x\right) = 0, \tag{A.7}$$

$$h_+\left(P(x,a) - P_-^a(x), P_-^a(x)\right) = 0. \tag{A.8}$$

Using implicit derivation, some lengthy but straightforward algebra yields

$$\tfrac{\partial P}{\partial a}\left(x_0, 0\right) = \tfrac{2}{\pi}\left(\tfrac{32}{9\pi} + \tfrac{2x_0}{3}\cot\tfrac{3\pi x_0}{2} + (4 - 2x_0)\cot\tfrac{\pi x_0}{2}\right) \ , \tag{A.9}$$

which exists and is continuous for all $x_0 \in I_-$, and has a solution therein iff (A.3) is fulfilled. Then, it easily follows from Bolzano's theorem that (A.3) has indeed a solution in $\left(\frac{1}{2}, \frac{2}{3}\right) \subset I_-$. Finally, for all $x_0 \in I_-$,

$$\begin{aligned}\tfrac{\partial^2 P}{\partial x \partial a}\left(x_0, 0\right) =& \tfrac{4}{\pi}\left(\tfrac{1}{3}\cot\tfrac{3\pi x_0}{2} - \cot\tfrac{\pi x_0}{2}\right) \\ & - 2x_0 \operatorname{cosec}^2\tfrac{3\pi x_0}{2} - (4 - 2x_0)\operatorname{cosec}^2\tfrac{\pi x_0}{2} < 0 \ ,\end{aligned} \tag{A.10}$$

and the result follows. □

**Lemma 10.** *For all $a \in (0, a_l) \subset \mathbb{R}^+$, there exists $\mu(a) \in \mathbb{R}^+$, $0 < \mu(a) \ll 1$, such that*

$$0 < \frac{\partial P}{\partial x}(x(a), a) < 1, \quad \forall x \in \left(x(a) - \mu(a), x(a) + \mu(a)\right), \tag{A.11}$$

*where $x = x(a)$ denotes the function defined by $P(x,a) - (x+4) = 0$.*

*Proof.* Taking implicit derivation with respect to $x$ in (A.7)-(A.8), combining both expressions for $x = x(a)$, recalling that $P(x(a), a) = 4 + x(a)$, and using the sine triple-angle identity, it follows that

$$\frac{\partial P}{\partial x}(x(a), a) = \frac{3 - 4\sin^2 \frac{\pi P_-^a((x(a))}{2}}{3 - 4\sin^2 \frac{\pi x(a)}{2}} e^{-4a}. \tag{A.12}$$

Moreover, it follows from (25) that $P_-^0(x) = 4 - x$; hence, by continuity there exists $\mu(a) \in \mathbb{R}$, $|\mu(a)| \ll 1$, such that $P_-^a(x) = 4 - x(a) + \mu(a)$, and (A.12) becomes

$$\frac{\partial P}{\partial x}(x(a), a) = \frac{3 - 4\sin^2 \frac{\pi x(a)}{2} + \pi\mu(a)\sin \pi x(a)}{3 - 4\sin^2 \frac{\pi x(a)}{2}} e^{-4a} + O\left(\mu^2(a)\right). \tag{A.13}$$

Then, substituting $x = x(a)$ and $P_-^a(x) = 4 - x(a) + \mu(a)$ into (A.7) and using Taylor expansions up to first order results in

$$\mu(a)\sin \pi x(a) = -8a \frac{\sin \pi x(a) + (2 - x(a))\left(\pi \cos^2 \frac{\pi x(a)}{2} - a \sin \pi x(a)\right)}{\pi^2 - 4a^2}. \tag{A.14}$$

Since $x(a) \in I_- = \left(0, \frac{2}{3}\right)$ this therefore implies that

$$\mu(a)\sin \pi x(a) \to 0^- \quad \text{when} \quad a \to 0^+, \tag{A.15}$$

and (A.11) follows directly. □

Theorem 1 is an immediate consequence of Lemma 9 and Lemma 10.

*Appendix A.2. Proof of Theorem 2*

According to Figure 2, a solution starting at $(x_0, y_0) = \left(\frac{10}{3}, 0\right)$ evolves on $S_+$. Using the function $P_+^a$ defined in (18), let

$$P_+^a(x_0) = P_+^a\left(\tfrac{10}{3}\right) \tag{A.16}$$

be the next crossing point of $S_0$.

**Lemma 11.** *For all $a \in \mathbb{R}^+$ we have that*

$$P_+^a\left(\tfrac{10}{3}\right) \in \left(4, \tfrac{14}{3}\right). \tag{A.17}$$

*Moreover there exist $a_1, \delta_1 \in \mathbb{R}^+$, $a_1 \gg 1$, $0 < \delta_1 \ll 1$, such that for all $a \in (a_1, +\infty)$, we have $P_+^a\left(\frac{10}{3}\right) \in (4, 4 + \delta_1)$.*

*Proof.* Following (18) and (21), let

$$x_1 = P_+^a\left(\tfrac{10}{3}\right) = \tfrac{10}{3} + \bar{x}_1\ , \tag{A.18}$$

be the first positive $x$ at which

$$h_+\left(\bar{x}, \tfrac{10}{3}\right) = e^{-a\bar{x}} \sin\varphi_+\left(\tfrac{10}{3}\right) - \sin\left(\tfrac{3\pi\bar{x}}{2} + \varphi_+\left(\tfrac{10}{3}\right)\right) = 0\ , \tag{A.19}$$

where

$$\varphi_+\left(\tfrac{10}{3}\right) = \frac{3\pi\frac{10}{3}}{2} - \phi_+ = 5\pi - \phi_+ \equiv \pi - \phi_+\ . \tag{A.20}$$

We know from (17) that $\phi_+ \in \left(0, \frac{\pi}{2}\right)$, for all $a \in \mathbb{R}^+$, so

$$\varphi_+\left(\tfrac{10}{3}\right) \equiv \pi - \phi_+ \in \left(\tfrac{\pi}{2}, \pi\right) \quad \Rightarrow \quad \sin\varphi_+\left(\tfrac{10}{3}\right) > 0,\ \forall a \in \mathbb{R}^+\ . \tag{A.21}$$

Therefore

$$0 < h_+^\infty\left(\bar{x}, \tfrac{10}{3}\right) < h_+\left(\bar{x}, \tfrac{10}{3}\right) < h_+^0\left(\bar{x}, \tfrac{10}{3}\right) \tag{A.22}$$

in appropriate intervals, yielding $\bar{x}_\infty < \bar{x}_1 < \bar{x}_0$, where $\bar{x}_0$ and $\bar{x}_\infty$ denote the first positive zeros of $h_+^0\left(\bar{x}, \frac{10}{3}\right)$ and $h_+^\infty\left(\bar{x}, \frac{10}{3}\right)$, respectively.

Using (23) we have that

$$\left.\begin{array}{l} \bar{x} = \frac{4}{3} \quad (n=1), \\ \bar{x} = \frac{2(2n+1)}{3} + \frac{4\phi_+}{3\pi} - 2\frac{10}{3} \in \left(\frac{2}{3}, \frac{4}{3}\right) \quad (n=5) \end{array}\right\} \quad \Rightarrow \quad \bar{x}_0 = \tfrac{4}{3}, \tag{A.23}$$

while (24) yields

$$\bar{x} = \tfrac{2n}{3} + \tfrac{2\phi_+}{3\pi} - \tfrac{10}{3} \in \left(\tfrac{2}{3}, \tfrac{4}{3}\right) \quad (n=5) \quad \Rightarrow \quad \bar{x}_\infty = \tfrac{2}{3}\ . \tag{A.24}$$

Notice that the worst cases for the lower limit (lowest value for $\bar{x}_\infty$) and the upper limit (highest value for $\bar{x}_0$) have been selected. Then

$$\tfrac{2}{3} < \bar{x}_1 < \tfrac{4}{3} \quad \Rightarrow \quad 4 < x_1 < \tfrac{14}{3} \quad \Rightarrow \quad x_1 \in \left(4, \tfrac{14}{3}\right), \quad \forall a \in \mathbb{R}^+\ . \tag{A.25}$$

This also implies that

$$a \to +\infty \quad \Rightarrow \quad \bar{x}_1 \to \bar{x}_\infty^+ = \tfrac{2}{3}^+ \quad \Rightarrow \quad x_1 \to 4^+. \tag{A.26}$$

Then the existence of $a_1$ and $\delta_1$ are guaranteed by continuity. □

As can be seen from Figure 2, a solution starting at $(x_1, 0)$, with $x_1 = P_+^a\left(\frac{10}{3}\right) \in \left(4, \frac{14}{3}\right)$, will evolve in $S_-$. Hence, the next crossing point of $S_0$ is

$$P_-^a\left(x_1\right) = \left(P_-^a \circ P_+^a\right)\left(\tfrac{10}{3}\right)\ . \tag{A.27}$$

**Lemma 12.** *There exist $a_2, \delta_2 \in \mathbb{R}^+$, $a_2 \gg 1$, $0 < \delta_2 \ll 1$, such that for all $a \in (a_2, +\infty)$, we have that $P_-^a(x) \in (6, 6+\delta_2)$, for all $x \in (4, 4+\delta_1)$.*

*Proof.* It follows using a similar approach to that used in Lemma 11. □

An equivalent procedure implies that for $a \to 0^+$ there do not exist sliding periodic solutions, as $\left(P_-^a \circ P_+^a\right)\left(\frac{10}{3}\right) \to \frac{22}{3}^+$, and $x = \frac{22}{3}^+$ belongs to the crossing region $S_{0C}$ beyond $\left(\frac{20}{3}, \frac{22}{3}\right)$, which is the next sliding interval after $\left(\frac{8}{3}, \frac{10}{3}\right)$. This result is consistent with Theorem 1.

According to Figure 2, a solution starting at $(x_2, 0)$ with

$$x_2 = \left(P_-^a \circ P_+^a\right)\left(\tfrac{10}{3}\right) \in (6, 6+\delta_2) \ , \tag{A.28}$$

will evolve in $S_+$. Hence the next crossing point of $S_0$ is

$$P_+^a(x_2) = \left(P_+^a \circ P_-^a \circ P_+^a\right)\left(\tfrac{10}{3}\right) \ . \tag{A.29}$$

**Lemma 13.** *There exist $a_3, \delta_3 \in \mathbb{R}^+$, $a_3 \gg 1$, $0 < \delta_3 \ll 1$, such that for all $a \in (a_3, +\infty)$, we have that $P_+^a(x) \in \left(\frac{20}{3}, \frac{20}{3}+\delta_3\right)$ for all $x \in (6, 6+\delta_2)$.*

*Proof.* It follows using a similar approach to that used in Lemma 11. □

The first part of the statement of Theorem 2 follows from the successive application of Lemma 11 and Lemma 13, with $a_h = \max\{a_1, a_2, a_3\}$, because $\left(\frac{20}{3}, \frac{20}{3}+\delta_3\right) \subset \left(\frac{20}{3}, \frac{22}{3}\right)$, which is the next attractive sliding interval after $\left(\frac{8}{3}, \frac{10}{3}\right)$.

The finite time convergence follows immediately for solutions with $x_i \in \left(\frac{8}{3}, \frac{10}{3}\right)$, because this is an attractive sliding interval and a solution starting therein is such that $y(x, x_i) = 0$, $\forall x \in \left[x_i, \frac{10}{3}\right]$, so in at most a distance of $\frac{2}{3}$ in $x$ it reaches the periodic solution $y\left(x, \frac{10}{3}\right) = 0$.

For $x_i \in \left(\frac{10}{3}, \frac{10}{3}+\nu(a)\right)$, Lemma 11 and Lemma 13 and the continuous dependence of solutions on initial conditions then imply that, given $a > a_h$, there exists $\delta(\nu(a)) \in \mathbb{R}^+$, $0 < \delta(\nu(a)) \ll 1$, such that

$$\left(P_+^a \circ P_-^a \circ P_+^a\right)(x_i) \in \left(\tfrac{20}{3}, \tfrac{20}{3}+\delta(\nu(a))\right) \subset \left(\tfrac{20}{3}, \tfrac{22}{3}\right) \tag{A.30}$$

hence in this case the periodic solution is reached in at most a distance 4 in $x$.

*Appendix A.3. Proof of Theorem 3*

**Lemma 14.** *For all $a \in \mathbb{R}^+$ we have that*

$$P_+^a(4n-2) \in \left(4n-\tfrac{4}{3}, 4n-\tfrac{2}{3}\right), \ \forall n \in \mathbb{N}\setminus\{0\}, \tag{A.31}$$

$$P_-^a(4n) \in (4n+2, 4n+4), \ \forall n \in \mathbb{N}. \tag{A.32}$$

*Proof.* It follows using a similar approach to that used in Lemma 11. □

Due to the overlapping of sliding intervals and the fact that $a > 0$, non-sliding periodic solution candidates are solutions that cross $S_0$ on $x = 2n$, $n \in \mathbb{N}$, and evolve alternatively in $S_+$ and $S_-$. However, it follows immediately from Lemma 14 that solutions exiting $S_0$ at such points hit again $y = 0$ in less than two $x$-units in either case. Therefore, non-sliding periodic solutions cannot exist in this case.

*Appendix A.4. Proof of Theorem 4*

Let $y_d(0) = 0$. Therefore $y_d(x) > 0$ for all $x \in (0, x_a)$, with $x_a$ stemming immediately from (A.32) in Lemma 14: $x_a = P_-^a(0) - 0 \in (2, 4)$. Now, assume that $y_d(x)$ evolves on a sliding interval of the type (28b) once on $S_0$, exiting at $x = 4$. Then the result follows by periodicity.

*Appendix A.5. Proof of Theorem 5*

Any solution starting in $S_+$ hits $S_0$ in finite time, say $x = x_{T_a}$. First let $x_{T_a} \in \left(0, \frac{2}{3}\right)$. As this is a crossing interval the system will continue its evolution in $S_-$, hitting again $S_0$ in $x > 2$. Assume that this solution, $y(x)$, follows a sliding interval of the type (28b) once on $S_0$, then $y(4n) = 0$ for a certain $n \in \mathbb{N}$, and thus intersects the periodic solution described in Theorem 4. Then, according to Definition 5, $y(x)$ behaves identically to such a periodic solution from the value of $x$ at which they intersect, which is allowed by the periodicity of the vector field. Now notice that $x_{T_a} \notin \left(\frac{2}{3}, \frac{4}{3}\right)$, as this is a repelling sliding interval. Finally, let $x_{T_a} > \frac{4}{3}$: assuming that $y(x)$ follows a sliding interval of the type (28b) once on $S_0$, the result follows as in the case $x_{T_a} \in \left(0, \frac{2}{3}\right)$.

*Appendix A.6. Proof of Theorem 6*

In the discontinuous system the existence of a periodic orbit, given in Theorem 1, was proven in Lemma 9 and Lemma 10 using the contractivity of a Poincaré map $P(x,a) = P_+^a\left(P_-^a(x)\right)$ defined in (A.1) for $0 < a \ll 1$. For the regularized system we define an analogous map

$P_\epsilon(x,a) = \left(P^a_{\epsilon+} \circ P^a_{\epsilon-}\right)(x)$. We may decompose $P^a_-$ and $P^a_{\epsilon-}$ each into three components

$$P^a_{\epsilon-} := P^a_{\epsilon-,3} \circ P^a_{\epsilon-,2} \circ P^a_{\epsilon-,1} \ , \quad P^a_- := P^a_{-,3} \circ P^a_{-,2} \circ P^a_{-,1} \ , \tag{A.33}$$

as illustrated in Figure A.18. It is immediate that $\epsilon \to 0$ entails $P^a_{\epsilon-,k}, P^a_{-,k} \to \mathbb{I}$ for $k = 1, 3$, while $P^a_{\epsilon-,2} = P^a_{-,2}$, for all $\epsilon$. Standard results on the regularity of initial conditions and transversality guarantee that $P^a_{\epsilon-} \overset{\mathcal{C}^1}{\to} P^a_-$ for $\epsilon \to 0$. Defining similar component maps for $P^a_+$ and $P^a_{\epsilon+}$ we have also $P^a_{\epsilon+} \overset{\mathcal{C}^1}{\to} P^a_+$, which implies $P_\epsilon \overset{\mathcal{C}^1}{\to} P$ for $\epsilon \to 0$. The result then follows immediately from Theorem 1.

*Appendix A.7. Proof of Theorem 7*

According to Theorem 2, sliding periodic solutions in the discontinuous case have crossing and sliding sections. Following the proof of Theorem 6, the Poincaré maps $P$ and $P_\epsilon$ can be defined and expressed as a composition of a finite number of successive maps, each from intervals of crossing to crossing, from crossing to sliding, or from sliding to crossing. For the maps from crossing to crossing intervals, the discussion in the proof of Theorem 6 applies, which means that they are Lipschitz continuous, with Lipschitz constant independent of $\epsilon$. For maps from crossing to sliding, theorem 2.1 in [3] applies directly, thus guaranteeing that the Lipschitz constant is exponentially small in $\epsilon$.

*Appendix A.8. Proof of Theorem 8*

Trajectories from $V_\pm$ enter the switching layer through the $x$-intervals where the corresponding vector field points towards $V_0$. Following (42),

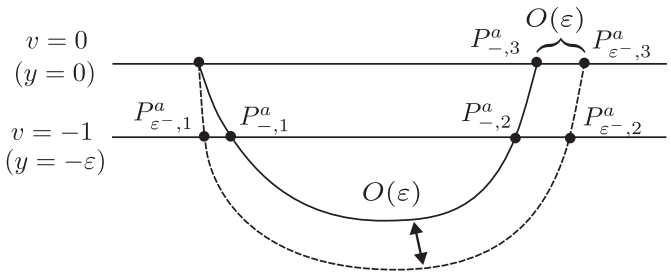


Figure A.18: The component mappings $P^a_{\epsilon-,k}$ and $P^a_{-,k}$ for $k = 1, 2, 3$.

these are

$$x \in \left(x^+_{\epsilon,4n}, x^+_{\epsilon,4n+2}\right) \quad \text{from} \quad V_+ \tag{A.34a}$$

$$x \in \left(x^-_{\epsilon,4n-2}, x^-_{\epsilon,4n}\right) \quad \text{from} \quad V_-. \tag{A.34b}$$

Hence, $V_0$ is accessed from $V_+$ between a stable and an unstable slow manifold, and from $V_-$ between an unstable and a stable manifold. The arrows in Figure 7 indicate the direction of the vector fields in $V_\pm$.

Let us first establish a result that will be used in the analysis of the dynamics of (51). Let $v_\pm\left(x, x_0^\pm\right)$ denote the solutions of (51) with initial conditions $\left(x_0^\pm, \pm 1\right)$. It is immediate that $v_\pm$ evolve on $V_\pm$ for $x_0^+ = x^+_{\epsilon,4n+2}$, $x_0^- = x^-_{\epsilon,4n}$, respectively, and eventually reach $V_0$ in finite time because of the fact that $a > 0$. It then makes sense, in the spirit of the map $P^a_\pm$ introduced in (18), to define $\bar{P}^a_{\epsilon\pm}(x)$ as the map providing the next intersection point of $v_\pm$ with $v = \pm 1$, respectively.

**Lemma 15.** *For all $n \in \mathbb{N}$, we have*

$$\bar{P}^a_{\epsilon+}\left(x^+_{\epsilon,4n+2}\right) \in \left(x^+_{\epsilon,4n+4}, x^+_{\epsilon,4n+6}\right) \tag{A.35a}$$

$$\bar{P}^a_{\epsilon-}\left(x^-_{\epsilon,4n}\right) \in \left(x^-_{\epsilon,4n+2}, x^-_{\epsilon,4n+4}\right). \tag{A.35b}$$

*Proof.* At $v = 1$, the vector field points towards $V_+$ on $\left(x^+_{\epsilon,4n+2}, x^+_{\epsilon,4n+4}\right)$ and towards $V_0$ on $\left(x^+_{\epsilon,4n+4}, x^+_{\epsilon,4n+6}\right)$, therefore $\bar{P}^a_{\epsilon+}\left(x^+_{\epsilon,4n+2}\right) > x^+_{\epsilon,4n+4}$. An analogous argument at $v = -1$ implies $\bar{P}^a_{\epsilon-}\left(x^-_{\epsilon,4n}\right) > x^-_{\epsilon,4n+2}$.

Now take initial states $x_0^+ = x^+_{\epsilon,4n+2}$ and $x_0^- = x^-_{\epsilon,4n}$. The solutions of (51) with initial conditions $\left(x_0^\pm, \pm 1\right)$ are

$$\begin{aligned} v_\pm\left(x, x_0^\pm\right) =& \frac{\omega_\pm \pi \cos\left(\omega_\pm \pi x\right) - a \sin\left(\omega_\pm \pi x\right)}{\epsilon\left(\omega_\pm^2 \pi^2 + a^2\right)} \\ & \pm e^{-a\left(x - x_0^\pm\right)} \left(1 + \frac{\omega_\pm \pi \sqrt{1 - a^2\epsilon^2} - a^2\epsilon}{\epsilon\left(\omega_\pm^2 \pi^2 + a^2\right)}\right). \end{aligned} \tag{A.36}$$

Letting $x_a^+ = x - x_0^+$, $x_a^- = x - x_0^-$, the conditions $v_\pm\left(x, x_0^\pm\right) = \pm 1$ result in

$$v_\pm\left(x, x_0^\pm\right) - (\pm 1) = \frac{\pm 1}{\omega_\pm^2 \pi^2 + a^2} h_\pm\left(x_a^\pm\right), \tag{A.37}$$

with

$$\begin{aligned} h_{\pm}\left(x_a^{\pm}\right) :=& a\left(\epsilon\omega_{\pm}\pi+\sqrt{1-a^2\epsilon^2}\right)\sin\left(\omega_{\pm}\pi x_a^{\pm}\right) \\ &-\left(\omega_{\pm}\pi\sqrt{1-a^2\epsilon^2}-a^2\epsilon\right)\cos\left(\omega_{\pm}\pi x_a^{\pm}\right)-\epsilon\left(\omega_{\pm}^2\pi^2+a^2\right) \\ &+e^{-ax_a^{\pm}}\left(\epsilon\omega_{\pm}^2\pi^2+\omega_{\pm}\pi\sqrt{1-a^2\epsilon^2}\right). \end{aligned} \tag{A.38}$$

It is clear that, for all $a,\epsilon\in\mathbb{R}^+$, with $a\epsilon\ll 1$,

$$h_u^{\pm}\left(x_a^{\pm}\right)>h_{\pm}\left(x_a^{\pm}\right), \tag{A.39}$$

where

$$\begin{aligned} h_u^{\pm}(z) :=& a\left(\epsilon\omega_{\pm}\pi+\sqrt{1-a^2\epsilon^2}\right)\sin\left(\omega_{\pm}\pi z\right) \\ &+\left(\omega_{\pm}\pi\sqrt{1-a^2\epsilon^2}-a^2\epsilon\right)\left[1-\cos\left(\omega_{\pm}\pi z\right)\right]. \end{aligned} \tag{A.40}$$

As, by construction, $h_{\pm}(z)>0$ when $z\to 0^+$, its first zero after $z=0$ is upper bounded by that of $h_u^{\pm}(z)$. Then it directly follows that

$$h_u^{\pm}(z)=0 \iff z_{\pm}=\frac{2m}{\omega_{\pm}},\ m\in\mathbb{Z}. \tag{A.41}$$

For $m=1$ this gives

$$x_a^{\pm}=x^{\pm}-x_0^{\pm}<\frac{2}{\omega_{\pm}} \tag{A.42}$$

and, recalling (42), one obtains

$$V_+:\ x^+<x^+_{\epsilon,4n+2}+\frac{4}{3}=x^+_{\epsilon,4n+6}, \tag{A.43}$$

$$V_-:\ x^-<x^-_{\epsilon,4n}+4=x^-_{\epsilon,4n+4}. \tag{A.44}$$

Hence, the result follows. □

Recall now the definition of $\Lambda_{0n}^N$ and $\Lambda_{\pm\delta n}^N$ in (55) and (56), respectively. Setting

$$\bar{\delta}=\sin\frac{3\pi\delta}{2}>a\epsilon, \tag{A.45}$$

it is immediate that

$$\sin\left(\pi x\left[1+\tfrac{1}{2}\psi(v)\right]\right)=\begin{cases} 0 & \forall\ (x,v)\in\Lambda_{0n}^N \\ \pm\bar{\delta} & \forall\ (x,v)\in\Lambda_{\pm\delta n}^N, \end{cases} \tag{A.46}$$

thus showing that $\Lambda^N_{0n}$ is enveloped by $\Lambda^N_{\pm\delta n}$, which are $\delta$-perturbations of $\Lambda^N_{0n}$ but are *not* invariant manifolds. Then, let $\mathcal{K}_{\delta n}$ be the compact set defined as

$$\mathcal{K}_{\delta n} := \left\{ (x,v) \in \mathbb{R}^2 : \; x \in \left[ \frac{4n}{3} + \delta, \frac{4n+2}{3} - \delta \right] \; \wedge \; |v| \leq 1 \right. \\ \left. \wedge \; \psi(v) \geq \frac{4n+3\delta}{x} - 2 \right\} . \tag{A.47}$$

Notice that, for all $(x,v) \in \mathcal{K}_{\delta n}$ and $\epsilon \to 0$, (51b) is such that

$$\dot{v} = -av - \frac{1}{\epsilon} \sin\left(\pi x \left[1 + \tfrac{1}{2}\psi(v)\right]\right) \leq a - \frac{1}{\epsilon}\bar{\delta} \xrightarrow[\epsilon \to 0]{} -\infty.$$

This means that the regular form of the vector field (51), i.e. (35), is pointing in the negative direction of the $v$ axis with infinite modulus, so $\mathcal{K}_{\delta n} \cap \Lambda^N_{\delta n}$ is reached in finite time. Then by regularity with respect to initial conditions and parameters, there exists $\epsilon_\delta = \epsilon_\delta(\delta) \in \mathbb{R}^+$ such that, for all $\epsilon \in (0, \epsilon_\delta)$, any trajectory starting within the subcompact set $\mathcal{K}_{2\delta n} \subset \mathcal{K}_{\delta n}$, where

$$\mathcal{K}_{2\delta n} := \left\{ (x,v) \in \mathbb{R}^2 : \; x \in \left[ \frac{4n}{3} + 2\delta, \frac{4n+2}{3} - 2\delta \right] \; \wedge \; |v| \leq 1 \right. \\ \left. \wedge \; \psi(v) \geq \frac{4n+3\delta}{x} - 2 \right\}, \tag{A.48}$$

evolves in $\mathcal{K}_{\delta n}$ and leaves it through the (upper) border of the compact set $\mathcal{V}_{2\delta n}$ defined in (58), where it arrives in finite time.

**Lemma 16.** *Let $a \in \mathbb{R}^+$ and $1 \gg \delta > 0$. Then there exist $\epsilon_\delta, \epsilon_+, \epsilon_- \in \mathbb{R}^+$ such that, $\forall n \geq 1$ and $\epsilon \in (0, \bar{\epsilon}_+)$, with $\bar{\epsilon}_+ = \min\{\epsilon_\delta, \epsilon_+, \epsilon_-\}$, the trajectories of (51) entering the switching layer $V_0$ from $V_+$ through $x \in \left(x^+_{\epsilon,4n}, x^+_{4n+2} - 2\delta\right)$ reach $\mathcal{V}_{2\delta n}$ in finite time, and keep evolving therein until they leave it by $x \geq 4n - 6\delta$.*

*Proof.* It follows from (32) and the compactness of $\mathcal{V}_{2\delta n}$ that $\psi'(v)$ has a positive lower bound in $\mathcal{V}_{2\delta n}$, namely, $L_{\psi'} = L_{\psi'}(\delta, n)$ such that $0 < L_{\psi'} \leq \psi'(v)$. Hence, there exists $\epsilon_\pm \in \mathbb{R}^+$ such that, for all $(x,v) \in \mathcal{V}_{2\delta n} \cap \Lambda^N_{\delta n}$ and $\epsilon \in (0, \epsilon_+)$ the flow is pointing downwards, i.e.

$$\vec{\nabla}\Lambda^N_{\delta n} \cdot (\dot{x}, \dot{y}) = 1 + \frac{\psi(v)}{2} - \frac{x\psi'(v)}{2\epsilon}\left(a\epsilon v + \sin\left(\pi x\left[1 + \tfrac{1}{2}\psi(v)\right]\right)\right) \leq \frac{3}{2} \\ - \frac{2n+3\delta}{3\epsilon}\psi'(v)\left(\bar{\delta} - a\epsilon\right) \leq \frac{3}{2} - \frac{2+3\delta}{3\epsilon}L_{\psi'}\left(\bar{\delta} - a\epsilon\right) \; < 0, \tag{A.49}$$

while a similar procedure implies that the flow is pointing upwards for all $(x,v) \in \mathcal{V}_{2\delta n} \cap \Lambda^N_{-\delta n}$ and $\epsilon \in (0, \bar{\epsilon}_-)$, with $\epsilon_- = \frac{\bar{\delta}}{a}$, hence

$$\vec{\nabla}\Lambda^N_{-\delta n} \cdot (\dot{x}, \dot{y}) > 1 + \frac{2+3\delta}{3\epsilon} L_{\psi'} \left(\bar{\delta} - a\epsilon\right) > 0. \tag{A.50}$$

Then for all $\epsilon \in (0, \min\{\epsilon_\delta, \epsilon_+, \epsilon_-\})$, any trajectory entering $\mathcal{V}_{2\delta n}$ evolves within this set and leaves it through the right border, namely $\mathcal{V}_{2\delta n} \cap \{(x,v) \in \mathbb{R}^2 : \ x = 4n - 6\delta\}$.

Recall now (40) and (42). As regards trajectories entering $V_0$ from $V_+$ by $\left(x^+_{\epsilon,4n}, x^+_{4n} + 2\delta\right)$, the vertical vector field component on $v = 1$ is negative, i.e. $\dot{v} < 0$, and $\dot{x} = 1$. Moreover, the vector field on $\Lambda^N_{-\delta n}$ is pointing upwards also for $x \in \left(x^+_{\epsilon,4n}, x^+_{4n} + 2\delta\right)$ and $\epsilon \in (0, \epsilon_-)$, as (A.50) holds in this region as well. Therefore, the trajectories within

$$\begin{aligned} \bar{\mathcal{K}}_{2\delta n} := \Big\{ (x,v) \in \mathbb{R}^2 : \ x \in \left(x^+_{\epsilon,4n}, x^+_{4n} + 2\delta\right) \ \wedge \ |v| \leq 1 \ \wedge \\ \wedge \ \psi(v) \geq \frac{4n - 3\delta}{x} - 2 \Big\}, \end{aligned} \tag{A.51}$$

are directed towards the left border of $\mathcal{K}_{2\delta n} \cup \mathcal{V}_{2\delta n}$, which is reached in finite time. □

**Remark 4.** *The trajectories entering the switching layer $V_0$ from $V_+$ through $x \in \left(\frac{4n+2}{3} - 2\delta, x^+_{\epsilon,4n+2}\right)$ will be either attracted to $\mathcal{V}_{2\delta n}$ or expelled again to $V_+$. However, a trajectory moving into $V_+$ with initial condition on $(x,v) = \left(x^+_{\epsilon,4n+2} + \alpha, 1\right)$, $1 \gg \alpha > 0$, is upper bounded by the one with initial condition $(x,v) = \left(x^+_{\epsilon,4n+2}, 1\right)$, and this one intersects again the line $v = 1$ within the (attractive) $x$-interval $\left(x^+_{\epsilon,4n+4}, x^+_{\epsilon,4n+6}\right)$, as shown in Lemma 15, so the trajectory starting on $(x,v) = \left(x^+_{\epsilon,4n+2} + \alpha, 1\right)$ will fall therein as well. If such entrance is by $x \in \left(x^+_{\epsilon,4n+4}, x^+_{4n+6} - 2\delta\right)$, then Lemma 16 applies and the trajectory is attracted by the corresponding $\mathcal{V}_{2\delta(n+1)}$, otherwise, the process is iterated and, eventually, only a set of solutions of small measure will not fall within $\left(x^+_{\epsilon,4n+4}, x^+_{4n+6} - 2\delta\right)$.*

An equivalent procedure implies the analogous result to Lemma 16 for trajectories entering $V_0$ from $V_-$.

**Lemma 17.** *Let $a \in \mathbb{R}^+$ and $1 \gg \delta > 0$. Then, given $1 \gg \hat{\delta} > 6\delta$, there exists $\bar{\epsilon}_- > 0$ such that, $\forall n \geq 1$ and $\epsilon \in (0, \bar{\epsilon}_-)$, the trajectories of (51) entering the switching layer $V_0$ from $V_-$ through $x \in \left(x^-_{\epsilon,4n-2}, x^-_{4n} - \hat{\delta}\right)$ reach $\mathcal{V}_{2\delta n}$ in finite time, and keep evolving therein until they leave it by $x \geq x^-_{4n} - 6\delta$.* □

The distance between the stable critical manifold $\Lambda^N_{0n}$ defined in (55) and its associated slow invariant manifold within $\mathcal{V}_{2\delta n}$, which is defined in (58), is given in next Lemma.

**Lemma 18.** *For all $n \geq 1$ and $1 \gg \delta > 0$, the trajectories of (51) evolving in the compact set $\mathcal{V}_{2\delta n}$, defined in (58), are exponentially attracted to a slow invariant manifold that, for all $x \in \left[\frac{5n}{3}, \frac{10n}{3}\right]$, is within $O\left(\frac{\epsilon}{n}\right)$ distance from the stable critical manifold $\Lambda^N_{0n}$ defined in (55).*

*Proof.* The (unique) formal expansion of the slow invariant manifold within $\mathcal{V}_{2\delta n}$ (see in (58)) assocciated to the stable critical manifold $\Lambda^N_{0n}$ (see (55)) in any subcompact of $\mathcal{V}_{2\delta n}$ sufficiently far from the fold points $\left(\frac{4n}{3}, 1\right)$ and $(4n, -1)$, where $\psi'(v) \neq 0$, is given by

$$v(x, \epsilon) = v_0(x) + \epsilon v_1(x) + O\left(\epsilon^2\right), \tag{A.52}$$

with $v_0(x)$ being such that $(x, v_0(x))$ stands for the graph of $\Lambda^N_{0n}$, i.e.

$$x\left(1 + \frac{\varphi(v_0(x))}{2}\right) = 2n. \tag{A.53}$$

Substituting (A.52) into (51b) while considering a Taylor expansion for the sinusoidal term in a neighbourhood of $v_0(x)$ and disregarding $O\left(\epsilon^2\right)$ terms yields

$$\dot{v}_0(x) + \epsilon \dot{v}_1(x) = -a\left(v_0(x) + \epsilon v_1(x)\right) - \frac{\pi x \varphi'(v)}{2}. \tag{A.54}$$

Then for $\epsilon \to 0$,

$$v_1(x) = 2\frac{\dot{v}_0(x) + a v_0(x)}{\pi x \psi'(v)}. \tag{A.55}$$

Let us now consider a compact subset of $\left[\frac{4n}{3} + 2\delta, 4n - 6\delta\right]$ where $v_0(x)$ has a 'flat' shape, i.e. far enough from $v = \pm 1$, say $\left[\frac{5n}{3}, \frac{10n}{3}\right]$. It is immediate that $v_0(x)$, $\dot{v}_0(x)$, and $\psi'(v_0(x))$ are bounded therein, so it follows straightforwardly that

$$v_1(x) \sim O\left(\tfrac{1}{x}\right) \sim O\left(\tfrac{1}{n}\right), \quad \forall x \in \left[\tfrac{5n}{3}, \tfrac{10n}{3}\right]. \tag{A.56}$$

Consequently, (A.52) implies

$$v(x) - v_0(x) \sim O\left(\tfrac{\epsilon}{n}\right), \quad \forall x \in \left[\tfrac{5n}{3}, \tfrac{10n}{3}\right]. \tag{A.57}$$

Then, Fenichel theory [8] and the preceding discussion yield the result. □

The $O\left(\frac{\epsilon}{n}\right)$-closeness between the stable critical manifold and the slow invariant manifold is lost in a neighbourhood of the fold points, where $\psi'(v)$ approaches zero and the graph of $v_0(x)$ loses the 'flat' shape. The next result studies the distance between the fold points, i.e. the ideal 'exiting points' of the switching layer, and the real exiting points, by turning (51) into a Riccati equation.

**Lemma 19.** *The trajectories of* (51) *trapped by an attractive slow invariant manifold leave* $V_0$ *by* $\left(\bar{x}^-_{\epsilon,4n}, -1\right)$*, with* $\bar{x}^-_{\epsilon,4n} \in \left(x^-_{\epsilon,4n}, x^-_{\epsilon,4n} + O\left(\left(\epsilon^2/n\right)^{\frac{1}{3}}\right)\right)$.

*Proof.* Using the change of variables

$$x - x^-_{\epsilon,4n} = \frac{\epsilon^{\frac{2}{3}}}{\alpha}\tilde{x}, \quad v + 1 = \frac{\pi\epsilon^{\frac{1}{3}}}{2\alpha^2}\tilde{v}, \quad t = \frac{\epsilon^{\frac{2}{3}}}{\alpha}\tau\,, \tag{A.58}$$

with

$$\alpha = \sqrt[3]{\frac{\pi}{2}\arcsin(a\epsilon) + \frac{n\pi^2\psi''(-1)}{2}}\,, \tag{A.59}$$

which is real because of (32c), system (51) can be written as

$$\dot{\tilde{x}} = 1, \tag{A.60a}$$

$$\dot{\tilde{v}} = -\left(\tilde{x} + \tilde{v}^2\right) + O\left(\frac{\epsilon^{2/3}}{n^{1/3}}\tilde{v}, \frac{\epsilon^{2/3}}{n^{1/3}}\tilde{x}^2, \frac{\epsilon^{2/3}}{n^{1/3}}\tilde{x}\tilde{v}, \epsilon^2\tilde{x}, \epsilon^2\tilde{v}\right). \tag{A.60b}$$

Neglecting the perturbative terms, (A.60) becomes a Riccati equation, which it is well known (see [22]) to have a unique, decreasing solution such that

$$\tilde{x} = -\tilde{v}^2 + O\left(1/\tilde{v}\right) \quad \text{as} \quad \tilde{v} \to +\infty, \tag{A.61}$$

$$\tilde{x} = \tilde{\Omega}_0 \quad \text{as} \quad \tilde{v} \to -\infty, \tag{A.62}$$

with $\tilde{\Omega}_0 \in \mathbb{R}^+$. This solution guides the deviation of the Fenichel manifold of the overall system (A.60) from the corresponding critical manifold, which is therefore bounded by some $\tilde{\Omega}$ such that $\tilde{\Omega}_0 < \tilde{\Omega}$. Hence, in the original variables we have that

$$x - x^-_{\epsilon,4n} < \tfrac{\epsilon^{2/3}}{\alpha}\tilde{\Omega} \quad \Rightarrow \quad \bar{x}^-_{\epsilon,4n} = x(-1) < x^-_{\epsilon,4n} + O\left(\left(\epsilon^2/n\right)^{\frac{1}{3}}\right). \tag{A.63}$$

Notice also that $\bar{x}^-_{\epsilon,4n} > x^-_{\epsilon,4n}$, which is consistent with the fact that for all $x \in \left(x^-_{\epsilon,4n-2}, x^-_{\epsilon,4n}\right)$ the vector field on $v = -1$ points upwards (i.e. towards $V_0$). $\square$

**Remark 5.** *Although it has not been necessary in the proof, an equivalent procedure would imply that the deviation of the slow invariant manifold from $x^+_{\epsilon,4n}$ on the upper boundary of $V_0$ is also $O\left(\left(\epsilon^2/n\right)^{\frac{1}{3}}\right)$.*

Finally, an analogous situation to that discussed in Remark 4 arises with the trajectories entering $V_-$ which are not guaranteed to reach $\mathcal{V}_{2\delta n}$, i.e., recalling Lemma 17, those entering through $x \in \left[x^-_{4n} - \bar{\delta}, x^-_{\epsilon,4n}\right)$. An equivalent reasoning implies that almost all of them will eventually catch up with a stable slow invariant manifold further on, and in any case none of them will ever reach $V_+$.

Figure A.19 illustrates the above analysis. Trajectories are in red, while vector field directions are in blue.

We are ready to prove item (i) of Theorem 8. It stems from Lemma 16 and Remark 4 that any trajectory with $x(0) = x_0 > 1$, $v(0) \geq 1$, except a set of small measure, intersects $v = 1$ with $x \in \left(x^+_{\epsilon,4n}, (4n+2)/3 - 2\delta\right)$ in finite time. Once in $V_0$, Lemma 18 ensures that it is exponentially trapped by a slow invariant (Fenichel) manifold and, according to Lemma 19, exits into $V_-$ by a point which is $O\left(\left(\epsilon^2/n\right)^{\frac{1}{3}}\right)$ to the right of $x^-_{\epsilon,4n} = 4n + 2\arcsin(a\epsilon)/\pi$. Hence, the minimum time that the trajectory remains in $V_0$ is

$$\begin{aligned}\Delta &= 4n + \frac{2}{\pi}\arcsin(a\epsilon) + O\left(\left(\epsilon^2/n\right)^{\frac{1}{3}}\right) - \left(\frac{4n+2}{3} - 2\delta\right) > \frac{8n - 2 + 6\delta}{3} \\ &= 2\left(\frac{4n+2}{3} - 2\delta\right) - 2 + 6\delta > 2\left(\frac{4n+2}{3} - 2\delta\right) - 2 > 2x_0 - 2.\end{aligned}$$

Let us now proceed with the proof of item (ii) in Theorem 8 by first defining the periodic object mentioned therein.

**Definition 7.** *Let $v_r(x)$ be the 4-periodic function defined as follows*

$$v_r(x) = v_-\left(x, x^-_{\epsilon,4n}\right), \quad x \in \left[x^-_{\epsilon,4n}, \bar{P}^a_{\epsilon-}\left(x^-_{\epsilon,4n}\right)\right], \tag{A.64a}$$

$$v_r(x) = -1, \quad x \in \left(\bar{P}^a_{\epsilon-}\left(x^-_{\epsilon,4n}\right), x^-_{\epsilon,4n+4}\right), \tag{A.64b}$$

*with $v_-(\cdot)$ denoting the solution of* (51) *with initial condition $\left(x^-_{\epsilon,4n}, -1\right)$ introduced in* (A.36).

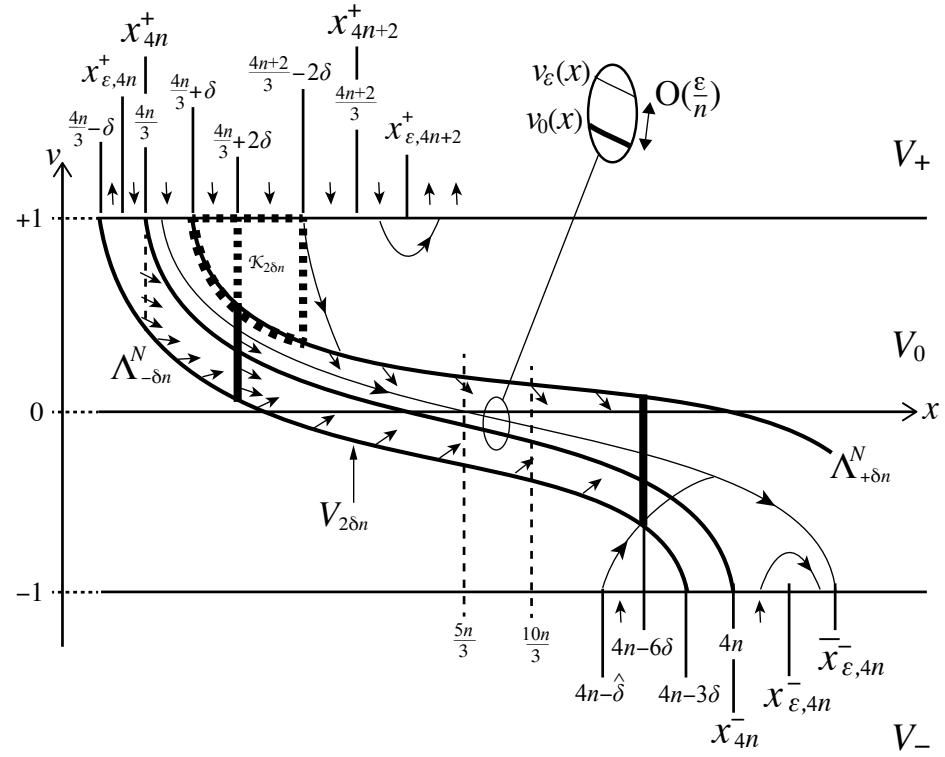


Figure A.19: Nonlinear regularization: dynamical analysis as described in the text. (Not to scale)

It follows from the previous discussion that most of the trajectories are eventually trapped by a slow invariant manifold within the switching layer and exit into $V_-$ at exponentially close distance to $\left(\bar{x}^-_{\epsilon,4n}, -1\right)$. Moreover, according to Lemma 15 and standard results on regularity of initial conditions and parameters, when $x > x^-_{\epsilon,4n+2}$ finds the vector field in $V_-$ pointing back towards $V_0$, so it is mapped again onto the switching layer at exponentially close distance from the entry point of the trajectory with initial condition $\left(\bar{x}^-_{\epsilon,4n}, -1\right)$, i.e $v_-\left(x, \bar{x}^-_{\epsilon,4n}\right)$, and lower bounded by the trajectory with initial condition $\left(x^-_{\epsilon,4n}, -1\right)$, i.e. $v_-\left(x, x^-_{\epsilon,4n}\right)$. Using $\bar{P}^a_{\epsilon-}$, such entry points are denoted as $\bar{P}^a_{\epsilon-}\left(\bar{x}^-_{\epsilon,4n}\right)$ and $\bar{P}^a_{\epsilon-}\left(x^-_{\epsilon,4n}\right)$, respectively, with Lemma 15, Lemma 19, (A.64a), regularity of initial conditions and the fact

that $a > 0$ indicating that:

$$0 < v_r(x) - v_-\left(x, \bar{x}^-_{\epsilon,4n}\right) < \mathcal{O}(\epsilon^{1/3}/n^{2/3}),\ x \in \left[\bar{x}^-_{\epsilon,4n}, \bar{P}^a_{\epsilon-}\left(\bar{x}^-_{\epsilon,4n}\right)\right], \quad \text{(A.65)}$$

and, in particular,

$$0 < \bar{P}^a_{\epsilon-}\left(x^-_{\epsilon,4n}\right) - \bar{P}^a_{\epsilon-}\left(\bar{x}^-_{\epsilon,4n}\right) < \mathcal{O}(\epsilon^{1/3}/n^{2/3}), \quad \text{with} \quad \text{(A.66a)}$$

$$\bar{P}^a_{\epsilon-}\left(\bar{x}^-_{\epsilon,4n}\right), \bar{P}^a_{\epsilon-}\left(x^-_{\epsilon,4n}\right) \in \left(x^-_{\epsilon,4n+2}, x^-_{\epsilon,4n+4}\right). \quad \text{(A.66b)}$$

Then both solutions enter $V_0$ and evolve therein upper bounded by the next (stable) Fenichel manifold, associated to $x^-_{4n+4}$, which acts as an upper bound. Consequently, they leave $V_0$ onto $V_-$ within $(x_{\epsilon,4n+4}, \bar{x}_{\epsilon,4n+4})$. After this, the process is repeated iteratively.

As $x \to +\infty$ is equivalent to $n \to +\infty$, it is then straightforward from (42) and (A.66) that, in such a case, $\bar{x}^-_{\epsilon,4n+4} \to x^-_{\epsilon,4n+4}$, $\bar{P}^a_{\epsilon-}\left(\bar{x}^-_{\epsilon,4n}\right) \to \bar{P}^a_{\epsilon-}\left(x^-_{\epsilon,4n}\right)$, and

$$v_-\left(x, \bar{x}^-_{\epsilon,4n}\right) \to v_r(x), \quad x \in \left[x^-_{\epsilon,4n}, \bar{P}^a_{\epsilon-}\left(x^-_{\epsilon,4n}\right)\right],$$

which, according to (A.64a), proves the statement in $v < -1$.

As for the behaviour of the continuation of the solution within $V_0$, a similar argument and regularity of initial conditions indicate that the solution starting at $\left(\bar{P}^a_{\epsilon-}\left(\bar{x}^-_{\epsilon,4n}\right), -1\right)$ tends to that staring at $\left(\bar{P}^a_{\epsilon-}\left(x^-_{\epsilon,4n}\right), -1\right)$, so we focus on this one within $(x_{\epsilon,4n+2}, x_{\epsilon,4n+4})$. However, notice that any $x \in (x_{\epsilon,4n+2}, x_{\epsilon,4n+4})$ can be written as

$$x = 4n + x_{\epsilon,a}, \quad \text{with } x_{\epsilon,a} \in \left(2 - \frac{2}{\pi}\arcsin(a\epsilon), 4 + \frac{2}{\pi}\arcsin(a\epsilon)\right).$$

Hence, the value of $\psi(v)$ at any $x \in (x_{\epsilon,4n+2}, x_{\epsilon,4n+4})$ for the $2n+4$ critical manifold is such that:

$$\psi(v)|_{x\in(x_{\epsilon,4n+2},x_{\epsilon,4n+4})} = 2\left(\frac{2(n+2)}{4n + x_{\epsilon,a}} - 1\right) \xrightarrow[n\to+\infty]{} -1.$$

This critical manifold is itself an upper bound for the Fenichel manifold that exists at $4(n+1)$, this yielding $v|_{x\in(x_{\epsilon,4n+2},x_{\epsilon,4n+4})} \to -1$.

Finally, notice that $\epsilon \to 0$ entails $x_{\epsilon,a} \in (2 - 2\arcsin(a\epsilon), 4) \to (2, 4)$, and $x^-_{\epsilon,4n} \to x^-_{4n} = 4n$. Hence, the function $y_r(x)$ obtained by reversing the change of variables $v = \frac{y}{\epsilon}$ for $v = v_r(x)$ is such that $y_r \to y_d$ for $\epsilon \to 0$, $y_d$ being the sliding 4-periodic solution of the discontinuous nonlinear system introduced in Theorem 4.

**Acknowledgments**

The authors gratefully thank the anonymous referees for their valuable suggestions and comments. J.M.O. was partially supported by the Government of Spain through the *Agencia Estatal de Investigación* Project DPI2017-85404-P and by the Generalitat de Catalunya through the *AGAUR* Project 2017 SGR 872. C.B. was partially supported by the Spanish government grant PGC2018-098676-B-I00. P.M. was partially supported by the Spanish government grant PGC2018-100928-B-I00. C.B. and P.M. were partially supported by the Catalan government grant 2017-SGR-1049.

**References**

[1] J. Awrejcewicz and D. Sendkowski. Stick-slip chaos detection in coupled oscillators with friction. *International Journal of Solids and Structures*, 42:5669–5682, 2005.

[2] C. Bonet, T. M. Seara, E. Fossas, and M. R. Jeffrey. A unified approach to explain contrary effects of hysteresis and smoothing in nonsmooth systems. *Commun. Nonlin. Sci. Numer. Simul.*, 50:142–68, 2017.

[3] C. Bonet-Revés and T. M. Seara. Regularization of sliding global bifurcations derived from the local fold singularity of Filippov systems. *Discrete and Continuous Dynamical Systems*, 36(7):3545–3601, 2016.

[4] B. Brogliato. *Nonsmooth mechanics – models, dynamics and control.* Springer-Verlag (New York), 1999.

[5] A. Colombo and M. R. Jeffrey. The two-fold singularity: leading order dynamics in n-dimensions. *Physica D*, 263:1–10, 2013.

[6] A. R. Crowther and R. Singh. Identification and quantification of stick-slip induced brake groan events using experimental and analytical investigations. *Noise Control Engineering Journal*, 56(4):235–255, 2008.

[7] M. di Bernardo, C. J. Budd, A. R. Champneys, and P. Kowalczyk. *Piecewise-Smooth Dynamical Systems: Theory and Applications.* Springer, 2008.

[8] N. Fenichel. Geometric singular perturbation theory. *J. Differ. Equ.*, 31:53–98, 1979.

[9] A. F. Filippov. *Differential Equations with Discontinuous Righthand Sides*. Kluwer Academic Publ. Dortrecht, 1988 (Russian 1985).

[10] M. H. Fredriksson and A. B. Nordmark. On normal form calculations in impact oscillators. *Proc. R. Soc. A*, 456:315–329, 2000.

[11] N. Hinrichs, M. Oestreich, and K. Popp. Dynamics of oscillators with impact and friction. *Chaos, Solitons & Fractals*, 8(4):535–558, 1997.

[12] N. Hinrichs, M. Oestreich, and K. Popp. On the modelling of friction oscillators. *J. Sound Vib.*, 216(3):435–459, 1998.

[13] C. Hös and A. R. Champneys. Grazing bifurcations and chatter in a pressure relief valve model. *Physica D*, 241(22):2068–76, 2012.

[14] J. Ing, E. Pavlovskaia, M. Wiercigroch, and S. Banerjee. Bifurcation analysis of an impact oscillator with a one-sided elastic constraints near grazing. *Physica D*, 239:312–321, 2010.

[15] M. R. Jeffrey. The ghosts of departed quantities in switches and transitions. *SIAM Review*, 60(1):116–36, 2017.

[16] Mike R. Jeffrey. *Hidden Dynamics: The mathematics of switches, decisions, & other discontinuous behaviour*. Springer, 2019.

[17] H. Jiang, A. S. E. Chong, Y. Ueda, and M. Wiercigroch. Grazing-induced bifurcations in impact oscillators with elastic and rigid constraints. *International Journal of Mechanical Sciences*, 127:204–14, 2017.

[18] P. Kowalczyk and P.T. Piiroinen. Two-parameter sliding bifurcations of periodic solutions in a dry-friction oscillator. *Physica D: Nonlinear Phenomena*, 237(8):1053 – 1073, 2008.

[19] Yu. A. Kuznetsov, S. Rinaldi, and A. Gragnani. One-parameter bifurcations in planar Filippov systems. *Int. J. Bif. Chaos*, 13:2157–2188, 2003.

[20] R. I. Leine and H. Nijmeijer. *Dynamics and Bifurcations of Non-Smooth Mechanical Systems*, volume 18 of *Lecture Notes in Applied and Computational Mathematics*. Springer, 2004.

[21] J. D. Meiss. *Differential Dynamical Systems*. SIAM, 2007.

[22] N.K. Mishchenko, E.F. Rozov. *Differential Equations with Small Parameters and Relaxation Oscillations*. Plenum Press, NY, 1980.

[23] D. N. Novaes and M. R. Jeffrey. Regularization of hidden dynamics in piecewise smooth flow. *J. Differ. Equ.*, 259:4615–4633, 2015.

[24] J. Palis and W. de Melo. *Geometric theory of dynamical systems*. Springer-Verlag, 1982.

[25] S. W. Shaw. On the dynamics response of a system with dry friction. *J. Sound Vib.*, 108(2):305–325, 1986.

[26] S. W. Shaw and P. J. Holmes. Periodically forced linear oscillator with impacts: Chaos and long-period motions. *PRL*, 51:623–626, 1983.

[27] J. Sotomayor and M. A. Teixeira. Regularization of discontinuous vector fields. *Proceedings of the International Conference on Differential Equations, Lisboa*, pages 207–223, 1996.

[28] Various. Special issue on dynamics and bifurcations of nonsmooth systems. *Physica D*, 241(22):1825–2082, 2012.

[29] B. A. Wernitz and N. P. Hoffman. Recurrence analysis and phase space reconstruction of irregular vibration in friction brakes: Signatures of chaos in steady sliding. *J. Sound Vib.*, 331:3887–96, 2012.